Report No. 71-3

STRUCTURES AND MATERIALS RESEARCH
DEPARTMENT OF CIVIL ENGINEERING

COMPARISON OF EXPERIMENTAL AND THEORETICAL RESPONSES IN HOLLOW RODS TO A TRANSIENT INPUT

by
G. PERNICA
and
H.D. McNIVEN

Report to
National Science Foundation
NSF Grant GK 10070

March 1971

STRUCTURAL ENGINEERING LABORATORY
UNIVERSITY OF CALIFORNIA
BERKELEY CALIFORNIA

Structures and Materials Research
Department of Civil Engineering
Division of Structural Engineering and Structural Mechanics

Report No. 71 - 3

COMPARISON OF EXPERIMENTAL AND THEORETICAL RESPONSES IN HOLLOW RODS TO A TRANSIENT INPUT

by

G. Pernica
Research Assistant
University of California
Berkeley, California 94720

and

H. D. McNiven
Professor of Engineering Science
University of California
Berkeley, California 94720

Structural Engineering Laboratory
University of California
Berkeley, California, 94720

March, 1971

I. INTRODUCTION

The method of characteristics has been used frequently in the last few years [1,2] to predict the response (usually measured as strains) at stations close to the end of a rod to an input imposed on the end of the rod. The method is capable of handling an input having any prescribed distribution in the radial direction and any time dependency. As the method admits problems dependent on only two independent variables (at least without considerable difficulty), it is usually necessary to employ an approximate theory in conjunction with the method.

Until now, the responses predicted by the method of characteristics have only been compared with other theoretical predictions, usually those obtained using integral transforms. These comparisons have been helpful in appraising the method of characteristics as a useful numerical technique. However, they shed no light in determining whether the approximate theory used in modeling the true physical system is actually appropriate. One way to obtain a worthy appraisal of an approximate theory and to establish further the suitability of the method of characteristics as a numerical technique is to compare the computed responses to actual experimental responses. That few such comparisons have until now been made is not without reason. The most important reason stems from the experiment itself.

Experimental responses arising from disturbances on the end of a rod have been recorded for inputs induced by a variety of devices. The strain history at a particular station or stations is usually measured accurately and displayed on an oscilloscope from which it

is photographed. The problem in using the experimental results (for comparison purposes) arises, not from the responses which are recorded in detail, but from the input which induced the response. As the device used to strike the end of the rod is known, it is usually straightforward to decide what variable (commonly stress) is to be used to fully describe the input and what spacial dependency is to be assumed for this variable at the input end. The difficulty encountered with the input is in knowing its time dependency.

The general nature of the time dependency can be surmised from the nature of the impacting device but this formulation is not good enough to use as an input with a theoretical method (approximate theory and numerical procedure) for appraising the method as a predictor of responses. The time histories of responses recorded experimentally are usually detailed and complex, requiring a time history of the input that is detailed and complex for a theoretical method to be fairly tested.

A method is devised here for testing a theoretical method (approximate theory and method of characteristics) as a predictor of responses against experimental results. The method requires that responses be recorded experimentally at two stations not far from one another. The response at station one (the station nearer the input end of the rod) is then treated as if it were an input. By considering this response as an input, the time dependency of the input (now in terms of strains) is known accurately. As responses can only be measured experimentally on the surface of the rod, the spacial dependency of the input must now be guessed at. The estimation of the spacial dependency could lead to serious difficulties in general,

but the difficulty is minimized here by considering tubes rather than solid rods. The radial dependency adopted for the input strains is that which satisfies the traction free conditions on the outer and inner surfaces of the tube, and for higher order theories, that which is consistent with the kinematic assumptions of the theory. The utilization of the experimental response at the first station as an input is, in fact, an exchange of time and spacial dependencies by which the complex time dependency is gained and the spacial dependency (which, for all but the thickest tubes, cannot be too different from the assumed spacial dependency) is lost. The response-input at station one is then used with the method of characteristics and an appropriate approximate theory to calculate the response at station two. The experimental and theoretical responses at station two are compared and the theoretical method appraised.

We are fortunate to have at our disposal the results of experiments conducted by Heimann and Kolsky [3,4]. We use the results of experiments conducted on tubes with two different ratios (a^*) of outer to inner radii. The data on the tube with $a^* = 1.03$ is obtained from reference [3] and the data on the tube with $a^* = 1.15$ from a report by Heimann [4]. The material of both tubes is reported to be of "cold drawn steel". Strains are induced in the tubes by holding the tubes in a vertical position and allowing a piece of a matching tube to suddenly drop on the specimen under study. For both tubes, stations one and two are 32" and 64" respectively from the impact end of the tube. The longitudinal strain ε_{zz}, and the hoop strain $\varepsilon_{\theta\theta}$, are measured on the outer lateral surface of each tube at both stations. The experimental results are particularly useful

as the authors were able to induce responses with complex time dependencies at both stations.

However, what is not so fortunate is that the experiments do not cover a large range of values of a*. One can predict that when the tube is thin (large radius/thickness ratio or a* in the neighborhood of 1), membrane theory will be adequate as the approximate theory to be used with the method of characteristics. This fact is demonstrated in the body of the paper. One can also predict that as the value of a* increases, a two-mode theory will give better results than membrane theory and, for even larger values of a*, a three-mode theory [5] will be an improvement on both. Unfortunately these latter predictions remain largely unanswered.

The hypothesis in this paper is that for a certain range of a* values a two-mode theory is the most appropriate and indeed, a two-mode theory is derived for the first time. However, the thicker of the two tubes for which a comparison is drawn, has an a* value which is in the region between those values for which membrane theory is adequate and those for which the two-mode theory would give improved predictions. Three-mode theory would not be needed for better predictions until the values of a* are much larger than those of the two tubes tested.

II. APPROXIMATE THEORIES FOR AXISYMMETRIC MOTIONS IN AN ISOTROPIC ELASTIC HOLLOW ROD

II-1. General Field Equations

Of the three approximate theories covered in this section only one is new; namely, two-mode theory. Both membrane theory and three-mode theory are well known and are reviewed here merely for completeness.

The semi-infinite tube is referred to a cylindrical co-ordinate system (r, θ, z). The origin of the system is located on the longitudinal axis at the end of the tube. The positive z axes and the axis of the tube coincide. The tube's outer radius is denoted by "b" and the inner radius by "a".

Because the field equations for a linear isotropic elastic material are common to all three theories we begin by setting down these equations. As the deformations are axisymmetric, we may assume the displacement field in the form

$$\begin{aligned} u_r &= u_r(r, z, t) \\ u_z &= u_z(r, z, t) \\ u_\theta &= 0 \end{aligned} \qquad (1)$$

Using small displacement gradient theory, the strain-displacement relations in cylindrical co-ordinates become

$$\begin{aligned} \varepsilon_{rr} &= u_{r,r} & \varepsilon_{r\theta} &= 0 \\ \varepsilon_{\theta\theta} &= \frac{u_r}{r} & \varepsilon_{rz} &= \frac{1}{2}(u_{z,r} + u_{r,z}) \\ \varepsilon_{zz} &= u_{z,z} & \varepsilon_{\theta z} &= 0 \end{aligned} \qquad (2)$$

The constitutive relation for a linear isotropic elastic material is

$$\tau_{ij} = 2\mu\varepsilon_{ij} + \delta_{ij}\lambda\Theta \tag{3}$$

where μ and λ are Lame's constants and δ_{ij} is the Kronecker delta.

With Eq. (2) and Eq. (3), stress components $\tau_{r\theta}$ and $\tau_{\theta z}$ are zero throughout the body. Thus, the stress equations of motion, omitting body forces, become

$$\begin{aligned} \tau_{rr,r} + \tau_{rz,z} + \frac{\tau_{rr} - \tau_{\theta\theta}}{r} &= \rho\ddot{u}_r \\ \tau_{rz,r} + \tau_{zz,z} + \frac{\tau_{rz}}{r} &= \rho\ddot{u}_z \end{aligned} \tag{4}$$

where $\dot{(\ )} = \frac{\partial(\ )}{\partial t}$ and ρ is the mass density. The third equation is satisfied identically.

II-2. Membrane Theory

Membrane theory begins with the kinematic assumptions that

$$\begin{aligned} u_r(r, z, t) &= u(z, t) \\ u_z(r, z, t) &= w(z, t) \end{aligned} \tag{5}$$

and the stress assumptions that

$$\tau_{rr} = \tau_{rz} = 0 \tag{6}$$

throughout the body.

When energy considerations are combined with the above assumptions and the field equations, the resulting equations of motion are

$$-\frac{an_\theta}{\mu} = \frac{\delta^2 A}{2} u_{,\tau\tau}$$
$$\frac{an_z}{\mu}{}_{,x} = \frac{\delta A}{2} w_{,\tau\tau} \quad . \tag{7}$$

In Eqs. (7)

$x = \frac{\delta z}{a}$ is a dimensionless distance

$\tau = \frac{\delta t}{a}\left(\frac{\mu}{\rho}\right)^{\frac{1}{2}}$ is a dimensionless time

$u(x, \tau)$ and $w(x, \tau)$ are generalized displacements

and n_θ and n_z are generalized forces defined by

$$n_\theta = \int_1^{a^*} \tau_{\theta\theta}\, dy$$
$$n_z = \int_1^{a^*} \tau_{zz}\, y\, dy \tag{8}$$

where

$$y = \frac{r}{a}$$
$$a^* = \frac{b}{a}$$
$$A = a^{*2} - 1.$$

In addition, δ is a constant defined as the first non-zero root of

$$J_1(\delta a^*) Y_1(\delta) - J_1(\delta) Y_1(\delta a^*) = 0 \quad [5]$$

where J_1 is the Bessel function of the first kind and Y_1 is the Bessel function of the second kind.

The constitutive equations relating generalized displacements and generalized forces are

$$\left(\frac{a}{\mu}\right)n_\theta = \frac{4(k^2-1)}{k^2}\,\frac{2(a^*-1)}{(a^*+1)}\,u + \frac{2(k^2-2)}{k^2}\,\delta(a^*-1)w_{,x}$$

$$\left(\frac{a}{\mu}\right)n_z = \frac{4(k^2-1)}{k^2}\,\frac{\delta A}{2}\,w_{,x} + \frac{2(k^2-2)}{k^2}\,(a^*-1)u \qquad (9)$$

where $k^2 = \frac{2(1-\nu)}{(1-2\nu)}$ and ν is Poisson's Ratio.

Finally the strains are given in terms of the generalized displacements according to

$$\varepsilon_{zz} = \frac{\delta}{a}\,w_{,x}$$

$$\varepsilon_{\theta\theta} = \frac{u}{r}$$

$$\varepsilon_{rr} = -\frac{(k^2-2)}{k^2}\left(\frac{u}{r} + \frac{\delta}{a}\,w_{,x}\right) \qquad (10)$$

$$\varepsilon_{rz} = 0 \quad .$$

A unique solution will result when we specify

1) throughout the tube, the initial values of w, u and $\dot{w}$, $\dot{u}$

2) at the end of the tube, one member of the product $\dot{w}n_z$.

For free harmonic motions, the frequency equation, in dimensionless form, is

$$\Omega^2\left[\Omega^2 - (k^2-1)(4\zeta^2 - \Omega^2)\right] + \frac{16}{(\delta(a^*+1))^2}\left[(k^2-1)(2\zeta^2 - \Omega^2) + \zeta^2(k^2-2)\right] = 0 \qquad (11)$$

where ζ is the dimensionless wave propagation constant and Ω is the dimensionless angular frequency.

The dimensionless variables ζ and Ω are related to their corresponding dimensional counterparts γ and ω according to

$$\zeta = \frac{a\gamma}{\delta}$$
$$\Omega = \frac{\omega}{\omega_1^s} \qquad (12)$$

where $\omega_1^s = \frac{\delta V_2}{a}$ is the first axial shear cut-off frequency and $V_2 = \left(\frac{\mu}{\rho}\right)^{\frac{1}{2}}$ is the shear wave velocity. Equation (11) gives rise to two modes for real values of the wave propagation constant.

The solution of Eq. (11) is shown in Figs. 1 and 2 using the properties of the two tubes for which experimental data exist. The method used to establish the value of 0.275 for Poisson's ratio of the "cold drawn steel" is explained in Section V. It can be seen from these figures that the approximate frequency spectra match the first mode of the exact theory well only for very small values of the wave propagation constant. The matching of the second mode is over a somewhat more extensive range.

Membrane theory, however, is restricted in use to thin-walled shells. The governing assumptions have imposed this limitation.

II-3. Three-mode Theory

In this and in the following section, two shell theories are outlined for which no restrictions concerning the thickness of the tube are made. The first of these two approximate theories, three-mode theory, accommodates shear deformation, bending deformation, and

rotary inertia of the shell. The second, two-mode theory, accommodates only shear deformation.

Three-mode theory was developed by McNiven, Shah, and Sackman [5]. It is based on the kinematic assumption that the displacements can be expressed in the form

$$u_r(r, z, t) = \frac{r}{a} u_0(z, t)$$
$$u_z(r, z, t) = w_0(z, t) + (1 - A_{11}r^2) w_1(z, t) \tag{13}$$

where $A_{11} = \frac{2}{b^2 + a^2}$.

The theory is contained in the three generalized displacement equations of motion

$$\delta^2 k^2 w_{0,xx} + 2\delta n_1 (k^2 - 2) u_{0,x} + \frac{2X_0}{\mu A} = \delta^2 w_{0,\tau\tau}$$

$$\delta^2 k^2 A^2 w_{1,xx} + 6\delta B^2 n_2^2 u_{0,x} - 24 B n_2^2 w_1 + \frac{6B^2 X_1}{\mu A} = \delta^2 A^2 n_4^2 w_{1,\tau\tau} \tag{14}$$

$$\delta^2 B n_2^2 u_{0,xx} - 4\delta n_1 (k^2 - 2) w_{0,x} - 4\delta n_2^2 w_{1,x} - 8 n_1^2 (k^2 - 1) u_0$$

$$+ \frac{4R_0}{\mu A} = \delta^2 B n_3^2 u_{0,\tau\tau}$$

where

$$X_0 = \left[r\tau_{rz} \right]_a^b$$

$$X_1 = \left[r(1 - A_{11}r^2)\tau_{rz} \right]_a^b$$

$$R_0 = \left[\frac{r^2}{a} \tau_{rr} \right]_a^b$$

and $$B = a^{*2} + 1 \quad .$$

The n_i's ($i = 1, 4$) are adjustment factors introduced into the theory to compensate for the omission of higher order terms in the kinematic assumptions and for the prejudiced displacement patterns of the terms included. As undetermined coefficients they are used in matching the three spectral lines of the approximate theory to the lowest three spectral lines of the exact theory. The adjustment factors are functions only of a^* and Poisson's ratio.

The constitutive equations relating the generalized displacements and generalized forces are

$$\left(\frac{a}{\mu}\right) P_{r0} = 2An_1^2 (k^2 - 1)u_0 + \delta An_1 (k^2 - 2)w_{0,x}$$

$$\left(\frac{a}{\mu}\right) P_{z0} = An_1 (k^2 - 2)u_0 + \frac{1}{2} \delta Ak^2 w_{0,x}$$

$$\left(\frac{a}{\mu}\right) P_{z1} = \frac{\delta A 3k^2}{6B^2} w_{1,x} \qquad (15)$$

$$\left(\frac{a}{\mu}\right) Q_0 = \frac{AB}{4} n_2^2 \left[\delta u_{0,x} - \frac{4w_1}{B} \right]$$

where the generalized forces are defined by

$$P_{r0} = \int_1^{a^*} (\tau_{rr} + \tau_{\theta\theta}) y dy$$

$$P_{z0} = \int_1^{a^*} \tau_{zz} y dy$$

$$P_{z1} = \int_1^{a^*} y(1 - \frac{y^2}{B}) \tau_{zz} dy \qquad (16)$$

$$Q_0 = \int_1^{a^*} y^2 \tau_{rz} dy \quad .$$

The strains are given in terms of the generalized displacements according to

$$\varepsilon_{rr} = n_1 \frac{u_0}{a}$$

$$\varepsilon_{\theta\theta} = n_1 \frac{u_0}{a}$$

$$\varepsilon_{zz} = \frac{\delta}{a} w_{0,x} + \frac{\delta(1 - A_{11} r^2)}{a} w_{1,x} \qquad (17)$$

$$\varepsilon_{rz} = \frac{n_2 r}{2a} \left[\frac{\delta}{a} u_{0,x} - 2A_{11} a w_1 \right] \quad .$$

A unique solution will result when we specify

1) throughout the tube, the initial values of w_0, w_1, u_0 and $\dot{w}_0, \dot{w}_1, \dot{u}_0$

2) throughout the tube, one member of each of the three products $\dot{w}_0 X_0$, $\dot{w}_1 X_1$, $\dot{u}_0 R_0$

3) at the end of the tube, one member of each of the three products $\dot{w}_0 P_{z0}$, $\dot{w}_1 P_{z1}$, $\dot{u}_0 Q_0$.

In order to find the frequency equation, we substitute

$$u_0(x,\tau) = F_1 \cos \zeta x \exp i\Omega\tau$$

$$w_0(x,\tau) = F_2 \sin \zeta x \exp i\Omega\tau \qquad (18)$$

$$w_1(x,\tau) = F_3 \sin \zeta x \exp i\Omega\tau$$

$$R_0 = X_0 = X_1 = 0$$

into Eqs. (14). The solution of the frequency equation (Eq. (42), Reference [5]) for $a^* = 1.03$, $\nu = 0.275$ and $a^* = 1.15$, $\nu = 0.275$ is shown in Figures 3 and 4 respectively. Although it appears that the first and third modes of the approximate spectra match their exact three dimensional counterparts identically for the entire range $0 \leq \zeta \leq 0.8$, slight differences which cannot be observed (because of the scale size) exist. The second mode for either set of shell values does not fare as well. Discrepencies between the approximate and exact solutions begin at very small values of ζ and increase noticeably as ζ increases.

II-4. Two-mode Theory

A study of the exact frequency spectra shown in Fig. 3 of Reference [5] indicates the dependency of the cut-off frequency of the second mode on both Poisson's ratio and a^*. An increase or decrease in Poisson's ratio or a^* has the same effect on the cut-off frequency of the second mode.

The effect of the a^* dependency yields an interesting result. For small values of a^* the first and second mode cut-off frequencies

are close to one another, resulting in strong coupling between these two modes. As the cut-off frequency of the third mode is considerably higher, the influence of this mode and all higher modes on the lowest two modes is significantly less pronounced. As the a* values of the tubes for which experimental results exist fall into this category, it seems appropriate to develop a two-mode theory.

Two-mode theory is based on the same kinematic assumptions introduced by Mindlin and Herrmann for a solid rod [6]

$$u_r(r, z, t) = \frac{r}{a} u(z, t)$$
$$u_z(r, z, t) = w(z, t) \quad . \tag{19}$$

As the theory is developed in a manner similar to that used by Mindlin and McNiven [7] for a solid rod, no derivation of this theory is required here. The theory is contained in two generalized displacement equations of motion

$$\delta^2 B m_2^2 u_{,xx} - 4\delta m_1 m_4 (k^2 - 2) w_{,x} - 8 m_1^2 (k^2 - 1) u + \frac{4R}{A\mu} = \delta^2 B m_3^2 u_{,\tau\tau} \tag{20}$$

$$\delta^2 m_4^2 k^2 w_{,xx} + 2\delta m_1 m_4 (k^2 - 2) u_{,x} + \frac{2X}{A\mu} = \delta^2 m_5^2 w_{,\tau\tau}$$

where

$$R = \left[\frac{\tau_{rr} r^2}{a} \right]_a^b$$

$$X = \left[\tau_{rz} r \right]_a^b \quad .$$

The m_i's ($i = 1,5$) are adjustment factors introduced into the theory to compensate for the omission of higher order displacement terms in the kinematic assumptions. For this reason we replaced in our development $\frac{u}{a}$ by $m_1\frac{u}{a}$, $u_{,z}$ by $m_2 u_{,z}$, and $w_{,z}$ by $m_4 w_{,z}$ in the strain-energy-density and $\dot{u}$ by $m_3\dot{u}$ and $\dot{w}$ by $m_5\dot{w}$ in the kinetic-energy-density. The values of the adjustment factors will be determined so that the two spectral lines of this theory match as closely as possible the lowest two branches of the exact theory. The adjustment factors are functions only of Poisson's ratio and a^*.

The constitutive equations relating the generalized displacements and generalized forces are

$$\left(\frac{a}{\mu}\right)P_r = 2Am_1^2\,(k^2 - 1)u + \delta Am_1m_4\,(k^2 - 2)w_{,x}$$

$$\left(\frac{a}{\mu}\right)P_z = Am_1m_4\,(k^2 - 2)u + \frac{\delta Ak^2}{2}\,m_4^2 w_{,x} \qquad (21)$$

$$\left(\frac{a}{\mu}\right)Q = \frac{\delta AB}{4}\,m_2^2 u_{,x}$$

where the generalized forces are defined by

$$P_r = \int_1^{a^*} (\tau_{rr} + \tau_{\theta\theta})y\,dy$$

$$P_z = \int_1^{a^*} \tau_{zz}y\,dy \qquad (22)$$

$$Q = \int_1^{a^*} \tau_{rz}y^2\,dy \quad .$$

The strains are given in terms of the generalized displacements according to

$$\varepsilon_{rr} = m_1 \frac{u}{a}$$

$$\varepsilon_{\theta\theta} = m_1 \frac{u}{a}$$

$$\varepsilon_{zz} = \frac{\delta}{a} m_4 w_{,x} \tag{23}$$

$$\varepsilon_{rz} = \frac{\delta m_2 r}{2a^2} u_{,x} \quad .$$

A unique solution will result when we specify

1) throughout the tube, the initial values of w,u and $\dot{w}$,$\dot{u}$
2) throughout the tube, one member of each of the products $\dot{w}X$ and $\dot{u}R$
3) at the end of the tube, one member of each of the products $\dot{w}P_z$ and $\dot{u}Q$.

Substitution of

$$u(x,\tau) = D_1 \cos \zeta x \exp i\Omega\tau$$

$$w(x,\tau) = D_2 \sin \zeta x \exp i\Omega\tau \tag{24}$$

$$R = X = 0$$

into the equations of motion, Eqs. (20), yields the dimensionless form of the frequency equation for two-mode theory

$$c_1 (\delta\Omega)^4 - c_2 (\delta\Omega)^2 + c_3 = 0 \tag{25}$$

where

$$c_1 = m_3^2 m_5^2 B$$

$$c_2 = B\left[m_3^2 m_4^2 k^2 + m_2^2 m_5^2\right](\delta\zeta)^2 + 8m_1^2 m_5^2 (k^2 - 1) \qquad (26)$$

$$c_3 = (\delta\zeta)^2\left[8m_1^2 m_4^2 (3k^2 - 4) + Bm_2^2 m_4^2 k^2 (\delta\zeta)^2\right] .$$

Discussion of Adjustment Factors

The adjustment factors m_i $(i = 1,5)$ are introduced into the theory as undetermined coefficients so that they may be used to match the spectral lines of the approximate theory to the lowest two spectral lines of the exact theory. As there are five adjustment factors, five properties of one set must be set equal to five properties of the other. For the reasons outlined in [5,7] we choose to match the cut-off frequency of the second mode, the curvature of the second mode at cut-off frequency, two points on one spectral line and one on the other. Using these five properties it is found that no solution in general can be obtained for the five unknown adjustment factors. In fact, unless the number of unknown adjustment factors is reduced to two, with the remainder being set equal to one, no solution in general is possible.

Our approach is now focused on determining which of the ten combinations of two adjustment factors provides the best match between approximate and exact spectral lines. For each combination, the cut-off frequency of the second mode was used as one property. The curvature of the second mode at cut-off frequency and a point on either

spectral line were each used in conjunction with the cut-off frequency as the second property.

Results which were again obtained for $a^* = 1.03$, $\nu = 0.275$, and $a^* = 1.15$, $\nu = 0.275$ were qualitatively identical. Optimal matching is achieved by considering either m_4 or m_5 in conjunction with either m_1 or m_3 as the unknown coefficients. However, because of the presence of m_4 or m_5, a disturbance would no longer propagate in the shell with the dilatational velocity unless the value of m_4 or m_5 as determined from the matching was equal to one. (See Section III.) As the values of m_4 or m_5 were significantly different from one, it was decided to forego these excellent matches for a poorer one, but one in which the dilatational velocity of the disturbance is maintained. The best matching, maintaining the dilatational velocity, was therefore chosen. Values for m_1 and m_2 were obtained by matching the cut-off frequency of the second mode and the point on the first spectral line at $\zeta = 0.70$.

The solution of Eq. (25) for both tubes using the values calculated for m_1 and m_2 is shown in Figs. 5 and 6.

III. SOLUTION OF GOVERNING EQUATIONS OF APPROXIMATE THEORIES BY METHOD OF CHARACTERISTICS

III-1. Formulation of the Theoretical Problem

The study under consideration involves a comparison between the actual dynamic response of a hollow rod as determined from experimentation and the response of the same rod as predicted by three approximate theories; namely, membrane theory, two-mode theory and three-mode theory using the method of characteristics.

The theoretical problem posed is that of determining the strain responses for a tube, initially at rest, whose cylindrical surfaces are free of traction and whose end is subjected to a strain input that has an arbitrary dependence on time. Written in mathematical form and in terms of variables associated with the exact three-dimensional theory, the prescribed initial and boundary conditions for the tube are

$$\begin{aligned} u_r(r, z, 0) &= \dot{u}_r(r, z, 0) = 0 \\ u_z(r, z, 0) &= \dot{u}_z(r, z, 0) = 0 \end{aligned} \tag{27}$$

and

$$\begin{aligned} \tau_{rz}(b, z, t) &= \tau_{rz}(a, z, t) = 0 \\ \tau_{rr}(b, z, t) &= \tau_{rr}(a, z, t) = 0 \\ \varepsilon_{zz}(b, 0, t) &= f(t) \\ \varepsilon_{zr}(b, 0, t) &= \varepsilon_{zr}(a, 0, t) = 0 \end{aligned} \tag{28}$$

respectively, where $f(t)$ is the longitudinal strain response recorded at station one.

The longitudinal strain responses recorded at station one for $a^* = 1.03$ and $a^* = 1.15$ are shown in Fig. 7. Information is shown for a limited time after the arrival of the first disturbance but a time that admits the maximum strain. The remainder of each recorded pulse is omitted as the effect of the finite tube length is to superimpose reflections on all but the first recorded pulse. We also note that the longitudinal strain responses are continuous functions of time.

The exact values of the longitudinal strains are not shown in Fig. 7. An arbitrary scale size was selected when the experimental responses at station one and station two were magnified from the photographs.

As the conditions given in Eqs. (27) and Eqs. (28) are not suitable for direct use with an approximate theory, a transformation to appropriate initial and boundary conditions for each approximate theory is required. This is performed later in this section.

The mathematical problem is now well formulated. For each approximate theory we seek the solution of a set of governing differential equations subject to initial and boundary conditions prescribed by Eqs. (27) and Eqs. (28).

III-2. Method of Characteristics

The general method of characteristics is by this time classical knowledge and so will not be reviewed in detail here. However, it makes the development more complete by explaining that the method of characteristics is one of reducing a system of hyperbolic partial differential equations to a system of equations containing

two basic simpler forms, each of which is amenable to numerical analysis. The first of these forms is called the canonical equation and the second, the decay equation. They are not applicable everywhere on the space-time plane. The canonical form of a differential equation is valid only along lines belonging to its characteristic family which are not wave fronts. Along a characteristic line which is not a wave front all derivatives of the generalized displacements appearing in the canonical equation are continuous and differentiable. The use of the canonical form is further restricted to these characteristic lines or portions of these lines contained within the domain of the disturbed material. For systems of hyperbolic differential equations for which many wave fronts exist, it is the first wave front which defines the boundary between disturbed and undisturbed domains. As discontinuities in the derivatives of the displacement vector may occur across a characteristic line describing a wave front, it is necessary to develop the decay equation. Along the characteristic line which is a wave front, the canonical equation is replaced by the decay equation. The decay equation calculates the magnitudes of the discontinuities of the derivatives of the displacement vector across the wave front.

For the particular systems of second order partial differential equations considered here, two different reduction techniques are employed. The first, a general method [8], reduces the differential equations to first order by the introduction of new dependent variables. The second [1] deals with the second order differential equations directly.

Membrane theory exhibits the first reduction technique, while two-mode and three-mode theories display the the second.

III-3. Canonical Form of the Governing Differential Equations

III-3(a) Membrane Theory

The governing differential equations, Eqs. (7) and Eqs. (9), are transformed into a set of first order differential equations by the introduction of new dependent variables. The new variables are related to the old according to

$$\begin{aligned} u_1 &= u_{,\tau} \\ u_2 &= w_{,\tau} \\ u_3 &= w_{,x} \\ u_4 &= \frac{an_\theta}{\mu} \\ u_5 &= \frac{an_z}{\mu} \end{aligned} \qquad (29)$$

By taking into consideration the generated relationship

$$u_{3,\tau} = u_{2,x} \qquad (30)$$

and by differentiating the constitutive relationships Eqs. (9) with respect to τ, the governing differential equations can be rewritten in the general form

$$u_{i,\tau} + B_{ij} u_{j,x} = c_i \qquad (i,j = 1\text{-}5) \qquad (31)$$

where

$$(u_i) = (u_1, u_2, u_3, u_4, u_5)$$

$$(B_{ij}) = \begin{bmatrix} 0 & 0 & 0 & 0 & 0 \\ 0 & 0 & 0 & 0 & -\frac{2}{\delta A} \\ 0 & -1 & 0 & 0 & 0 \\ 0 & -\delta e^2 (a^* - 1) & 0 & 0 & 0 \\ 0 & -\frac{\delta f^2 A}{2} & 0 & 0 & 0 \end{bmatrix} \tag{32}$$

$$(c_i) = \begin{bmatrix} -\frac{2u_4}{\delta^2 A} \\ 0 \\ 0 \\ \frac{2f^2 (a^* - 1)}{(a^* + 1)} u_1 \\ e^2 (a^* - 1) u_1 \end{bmatrix} \tag{33}$$

and

$$e^2 = \frac{2(k^2 - 2)}{k^2}$$

$$f^2 = \frac{4(k^2 - 1)}{k^2} \quad .$$

In effect, what we have done is to replace the four governing differential equations, Eqs. (7) and Eqs. (9), governing the four unknown dependent variables w, u, n_z, and n_θ by a set of five differential equations, Eqs. (31), governing five new dependent variables u_1, u_2, u_3, u_4, and u_5.

To establish the canonical forms of Eqs. (31) it is necessary to determine the characteristic lines along which they are valid. The characteristic equation

$$\det(B_{ij} - \lambda_{ij}) = 0 \,, \tag{34}$$

where $\lambda = \frac{dx}{d\tau}$ defines the characteristic lines on the $(x - \tau)$ plane, yields the required information. The values of λ are

$$\lambda^{(1)} = f \qquad \lambda^{(2)} = -f \qquad \lambda^{(3)} = \lambda^{(4)} = \lambda^{(5)} = 0 \,. \tag{35}$$

We not that $\lambda = f$ and $\lambda = -f$ describe the two families of physical characteristics on the $(x - \tau)$ plane. These are the only lines across which the derivatives of the displacement vector may suffer a finite jump. The canonical forms of the governing equations are

$$h_m^{(i)} \frac{du_m}{d\tau} = h_m^{(i)} c_m \qquad \text{along } \frac{dx}{d\tau} = \lambda^{(i)} \qquad (i,m = 1 - 5) \tag{36}$$

where the $h_m^{(i)}$ is the i^{th} left-hand eigenvector of the matrix B.

In neither of the vectors $\{u_m\}$ or $\{c_m\}$ do the generalized displacements w or u appear explicitly. Their presence is not essential for the solution of stress-resultants or strains within the medium. However, it makes the solution of the problem more complete if they are included. The canonical forms of the governing equations, Eqs. (36), together with the differentiability conditions

$$\begin{aligned} du &= u_{,\tau} d\tau = u_1 d\tau \\ dw &= w_{,\tau} d\tau = u_2 d\tau \end{aligned} \qquad \text{along } x = \text{const.} \tag{37}$$

can be written as

$$\alpha_{ij} \frac{dv_j}{d} = \beta_{ij} v_j \qquad (i,j = 1 - 7) \qquad (38)$$

where

$$(v_j) = (u_1, u_2, u_3, u_4, u_5, w, u)$$

$i = 1,2$ along the characteristics $\frac{dx}{d\tau} = f, - f$

$i = 3 - 7$ along the lines $\frac{dx}{d\tau} = 0$

and

$$(\beta_{ij}) = \begin{bmatrix} 0 & \frac{\delta f A}{2} & 0 & 0 & -1 & 0 & 0 \\ 0 & \frac{\delta f A}{2} & 0 & 0 & 1 & 0 & 0 \\ 1 & 0 & 0 & 0 & 0 & 0 & 0 \\ 0 & 0 & \frac{\delta f^2 A}{2} & 0 & -1 & 0 & 0 \\ 0 & 0 & \delta e^2 (a^* - 1) & -1 & 0 & 0 & 0 \\ 0 & 0 & 0 & 0 & 0 & 1 & 0 \\ 0 & 0 & 0 & 0 & 0 & 0 & 1 \end{bmatrix} \qquad (39)$$

$$(\beta_{ij}) = \begin{bmatrix} -e^2(a^*-1) & 0 & 0 & 0 & 0 & 0 & 0 \\ e^2(a^*-1) & 0 & 0 & 0 & 0 & 0 & 0 \\ 0 & 0 & 0 & -\frac{2}{\partial^2 A} & 0 & 0 & 0 \\ -e^2(a^*-1) & 0 & 0 & 0 & 0 & 0 & 0 \\ -\frac{2f^2(a^*-1)}{(a^*+1)} & 0 & 0 & 0 & 0 & 0 & 0 \\ 0 & 1 & 0 & 0 & 0 & 0 & 0 \\ 1 & 0 & 0 & 0 & 0 & 0 & 0 \end{bmatrix} \quad (40)$$

The initial and boundary conditions are derived from Eqs. (27) and Eqs. (28). In terms of the components of the vector (v_j), the initial and boundary conditions are

$$u(x, 0) = u_1 (x, 0) = 0$$

$$w(x, 0) = u_2 (x, 0) = 0 \tag{41}$$

and

$$\frac{\delta}{a} u_3 (0, \tau) = f_1 (\tau)$$

respectively, where $f_1 (\tau)$ is the longitudinal strain recorded at station one. The above three conditions, Eqs. (41), satisfy the uniqueness criteria as specified for membrane theory in Section II.

We delay the discussion of the decay equation until the canonical forms of the governing equations and the initial and boundary conditions for two-mode and three-mode theories have been presented.

III-3(b) Two-mode Theory

This procedure begins by rewriting the governing equations, Eqs. (20), with R = X = 0 in the form

$$u_{i,xx} - \frac{1}{c_i^2} u_{i,\tau\tau} = \alpha_{ij} u_j + \beta_{ij} u_{j,x} \qquad (i,j = 1, \ldots, n) \quad \text{(no sum on i)} \tag{42}$$

where $\frac{dx}{d\tau} = \pm c_i$ defines the physical characteristic lines on the $(x - \tau)$ plane. For our particular set of equations, if we take

$$(u_1, u_2) = (w, u)$$

we obtain

$$(\alpha_{ij}) = \begin{bmatrix} 0 & 0 \\ 0 & \dfrac{8m_1^2\,(k^2-1)}{\delta^2 B m_2^2} \end{bmatrix} \tag{43}$$

$$(\beta_{ij}) = \begin{bmatrix} 0 & -\dfrac{2m_1\,(k^2-2)}{\delta k^2} \\ \dfrac{4m_1\,(k^2-2)}{\delta B n_2^2} & 0 \end{bmatrix} \tag{44}$$

and

$$c_1^2 = k^2 \qquad\qquad c_2^2 = m_2^2 \quad .$$

For the values of Poisson's ratio and a* considered here, it can be readily shown that

$$c_1^2 > c_2^2 \quad .$$

We note that $c_1 = k$ is the dimensionless form of the dilatational velocity $\dfrac{(\lambda + 2\nu)^{\frac{1}{2}}}{\rho}$.

The canonical form of Eqs. (42) along $\dfrac{dx}{d\tau} = \mp c_i$ is (Eqs. (16) Ref.[1])

$$\mp d(u_{i,x}) - \frac{1}{c_i} d(u_{i,\tau}) = \mp dx(\alpha_{ij}u_j + \beta_{ij}u_{j,x}) \qquad (i,j = 1,\ldots,n)$$

(no sum on i) (45)

Accordingly, the canonical forms of Eqs. (20) are

$$\mp d(w_{,x}) - \frac{1}{c_1} d(w_{,\tau}) = \mp dx\beta_{12}u_{,x} \qquad \text{along } \frac{dx}{d\tau} = \mp c_1$$

$$\mp d(u_{,x}) - \frac{1}{c_2} d(u_{,\tau}) = \mp dx(\alpha_{22}u + \beta_{21}w_{,x}) \qquad \text{along } \frac{dx}{d\tau} = \mp c_2 \quad . \tag{46}$$

Equation (46) is a set of four equations relating the five unknown dependent variables $w_{,x}$, $w_{,\tau}$, $u_{,x}$, $u_{,\tau}$, and u. To get the necessary fifth equation we exploit the fact that the displacement field is continuous and differentiable so that along any line on the $(x - \tau)$ plane not belonging to the families of physical characteristic lines the relationships

$$\begin{aligned} dw &= w_{,x}dx + w_{,\tau}d\tau \\ du &= u_{,x}dx + u_{,\tau}d\tau \end{aligned} \tag{47}$$

are always valid. (As the generalized displacement w does not appear explicitly in Eqs. (46), the first relationship given in Eqs. (47) can be omitted. It is included here in order to present a more detailed solution.) In particular, along the family of lines x = const. these relationships become

$$\begin{aligned} dw &= w_{,\tau}d\tau \\ du &= u_{,\tau}d\tau \quad . \end{aligned} \tag{48}$$

The set of canonical equations is now complete. Equations (46) and Eqs. (48) combine to form a system of six equations in the six unknown components of the vector

$$(v_j) = (w_{,x},\ w_{,\tau},\ u_{,x},\ u_{,\tau},\ w,\ u) \quad .$$

The initial and boundary conditions determined from Eqs. (27) and Eqs. (28) are, in terms of the components of the vector (v_j),

$$u(x, 0) = u_{,\tau}(x, 0) = 0$$

$$w(x, 0) = w_{,\tau}(x, 0) = 0$$

and (49)

$$\frac{\delta}{a} w_{,x}(0,\tau) = f_1(\tau)$$

$$u_{,x}(0,\tau) = 0$$

respectively. Examination of the uniqueness criteria stated in Section II reveals the adequacy of Eqs. (49).

III-3(c) Three-mode Theory

As the development of the canonical equations for three-mode theory is identical to that presented in the preceding section, it suffices merely to write down these equations. The canonical equations are

$$\mp d(w_{0,x}) - \frac{1}{c_1} d(w_{0,\tau}) = \mp dx\beta_{12}u_{0,x} \qquad \text{along } \frac{dx}{d\tau} = \mp c_1$$

$$\mp d(u_{0,x}) - \frac{1}{c_2} d(u_{0,\tau}) = \mp dx(\alpha_{32}u_0 + \beta_{31}w_{0,x} + \beta_{33}w_{1,x}) \qquad (50)$$

$$\text{along } \frac{dx}{d\tau} = \mp c_2$$

$$\mp d(w_{1,x}) - \frac{1}{c_3} d(w_{1,\tau}) = \mp dx(\alpha_{23}w_1 + \beta_{22}u_{0,x}) \qquad \text{along } \frac{dx}{d\tau} = \mp c_3$$

$$dw_0 = w_{0,\tau}\, d\tau$$

$$dw_1 = w_{1,\tau}\, d\tau \qquad \text{along } x = \text{const.} \qquad (51)$$

$$du_0 = u_{0,\tau}\, d\tau$$

where

$$(\alpha_{ij}) = \begin{bmatrix} 0 & 0 & 0 \\ 0 & 0 & \dfrac{24Bn_2^2}{\delta^2 A^2 k^2} \\ 0 & \dfrac{8n_1^2 (k^2 - 1)}{\delta^2 Bn_2^2} & 0 \end{bmatrix} \tag{52}$$

$$(\beta_{ij}) = \begin{bmatrix} 0 & -\dfrac{2n_1 (k^2 - 2)}{\delta k^2} & 0 \\ 0 & -\dfrac{6B^2 n_2^2}{\delta A^2 k^2} & 0 \\ \dfrac{4n_1 (k^2 - 2)}{\delta Bn_2^2} & 0 & \dfrac{4}{\delta B} \end{bmatrix} \tag{53}$$

and

$$c_1^2 = k^2 \qquad c_2^2 = \frac{n_2^2}{n_3^2} \qquad c_3^2 = \frac{k^2}{n_4^2}$$

For the Poisson's ratio and a*'s used here, it can be shown that

$$c_1^2 > c_2^2 > c_3^2 \ .$$

We again note that $c_1 = k$ is the dimensionless form of the dilatational wave velocity. Equations (50) and (51) form a system of nine equations in the nine unknown components of the vector

$$(v_j) = (w_{0,x}, w_{0,\tau}, w_{1,\tau}, u_{0,x}, u_{0,\tau}, w_0, w_1, u_0).$$

The initial and boundary conditions are again derived from Eqs. (27) and Eqs. (28). However, it is necessary to assume a form

for the radial dependency of the longitudinal strain at station one in order to fulfil the uniqueness criteria. Consistency with the kinematic assumptions of three-mode theory dictates the choice of a quadratic dependency. The kinematic assumptions do not in themselves dictate whether ε_{zz} increases or decreases as the radius increases. The choice made here is that the longitudinal strain increases.

Employing $g(r) = \frac{r^2}{b^2}$ as the radial dependency for the longitudinal strain at station one, the initial and boundary conditions for the tube are

$$w_0\,(x,\,0) = w_{0,\tau}\,(x,\,0) = 0$$

$$w_1\,(x,\,0) = w_{1,\tau}\,(x,\,0) = 0$$

$$u_0\,(x,\,0) = u_{0,\tau}\,(x,\,0) = 0$$

and (54)

$$2\,\frac{\delta}{a}\,w_{0,x}\,(0,\,\tau) = f_1\,(\tau)\left[\,g(a) + 1\,\right]$$

$$2\,\frac{A}{B}\,\frac{\delta}{a}\,w_{1,x}\,(0,\,\tau) = f_1\,(\tau)\left[\,g(a) - 1\,\right]$$

$$u_{0,x}\,(0,\,\tau) - \frac{4}{B}\,w_1\,(0,\,\tau) = 0$$

respectively.

III-4. Decay Equations

On the $(x - \tau)$ plane a wave front can be represented by a line and, by definition, that line will be a characteristic. For each approximate theory the initial conditions are all zero and the boundary conditions are continuous functions of τ, which imply that

of a single family of physical characteristic lines it is the one emanating from the origin of the $(x - \tau)$ plane that will be the wave front. Hence, membrane theory, two-mode theory and three-mode theory have one, two, and three wave fronts respectively. The magnitude of the jump of a derivative of the displacement vector across a characteristic line describing a wave front will depend on the boundary conditions on the end of the tube; specifically, the dependence on time in the neighborhood of $\tau = 0$.

If, at least one of the boundary conditions suffers a finite jump at $\tau = 0$, then some components of the vector (v_j) will suffer a jump across a wave front [1,9]. The specific components suffering the jump depend on the wave front considered if more than one wave front exists. For each approximate theory, all boundary conditions are continuous at $\tau = 0$. There is no need, therefore, to formally develop the decay equations for each theory. All components of the vector (v_j) for each approximate theory are continuous across all existing wave fronts.

IV. NUMERICAL ANALYSIS

IV-1. General Comments

We are interested in obtaining the longitudinal and hoop strain responses at station two, located 32" along the tube from station one. In order to determine these dynamic responses, it is necessary to establish, at station two, a finite set of vectors $\left\{ v_j\left(\frac{32\delta}{a} , \tau_m\right)\right\}$ ($m = 1,2,\ldots,s$; $s - 1$ = the number of time intervals desired). With the components of the vectors $\left\{ v_j\left(\frac{32\delta}{a} , \tau_m\right)\right\}$ known, the longitudinal and hoop strain responses are readily calculated.

The numerical technique employed to obtain the solution of the vectors $\left\{ v_j\left(\frac{32\delta}{a} , \tau_m\right)\right\}$ for the three approximate theories closely parallels the numerical method utilized by McNiven and Mengi in their papers [1,9]. Although the same numerical method is used with each of the approximate theories, the difference in the number of wave fronts exhibited by each of the three theories warrants the inclusion in this section of two separate descriptions of the method; one for membrane theory and the other for two-mode and three-mode theories.

IV-2. Membrane Theory

We refer to Fig. 8 which shows the $(x - \tau)$ plane. On this plane, the line T: $x - f\tau = 0$ divides the space-time domain into two parts; the domain D_1, representing undisturbed particles and D_2, representing particles of the body which are in motion. The part D_2, which is the part that interests us, is subdivided by means of

a grid. The grid shown by fine solid lines is formed by two sets of parallel lines. The first set ($x - f\tau$ = const.) is parallel to the line T and the second set ($x + f\tau$ = const.) has equal but opposite slopes. Each diamond-shaped element has diagonals measuring $2\Delta X$ and $2\Delta\tau$.

To establish $\left\{ v_j \left(\frac{32\delta}{a} , \tau_m \right) \right\}$ we start by prescribing values of (v_j) as determined by the decay equation to all nodal points along T, beginning with (1,1) and terminating with (1,n). The integer "n" is calculated from the equation

$$n = s + p$$

where s is an integer previously defined in this section and p is an integer determined from the equation

$$p = \frac{\frac{32\delta}{a}}{\Delta X} + 1 \quad .$$

We then proceed to the next characteristic line parallel to T. Using a procedure to be explained shortly [9], we determine the values of (v_j) for each of the required nodal points along this line, beginning with (2,1) and terminating with (2, n - 1). With (v_j) established along the second characteristic line, we then proceed to the third, the fourth, and so on, until s characteristic lines have been explored.

In explaining the technique we refer to element M shown in Fig. 9. The vector (v_j) is known at points B_3 and B_4 located on the b^{th} characteristic line and point C_2 located on the c^{th} characteristic line. As there are seven unknowns we need seven equations to establish them.

The seven equations come from using the canonical form of the

governing equations, Eqs. (38), along their respective characteristic lines. The seven elements of (v_j) are found at C_3 by solving the seven equations by the method of finite differences.

For the element L adjacent to the line $x = 0$, the procedure is the same except that the canonical equation along the line $x - f\tau = \text{const.}$ is replaced by the boundary condition at $x = 0$; namely, the last of Eqs. (41)

$$\frac{\delta}{a} u_3 (C_1) = f_1 (C_1) \quad . \tag{55}$$

As the time dependency of the input (station one) for each tube is very complex, no attempt is made to reproduce it in functional form. The longitudinal strain response at station one is magnified from the photographs and a set of descrete values of f(t) established graphically at intervals of t = 1.25 microseconds. By considering this set of discrete values as the input, the value of $f_1 (C_1)$ for any mesh size is determined by interpolating the elements of the input set quadratically.

IV-3. Two-mode Theory (Three-mode Theory*)

We refer to Fig. 9 which shows the $(x - \tau)$ plane divided into D_1 and D_2 domains by the line T_1: $x - c_1\tau = 0$. The domain D_2 is subdivided by means of one primary grid and one secondary grid (two secondary grids*). The primary grid shown by fine solid lines consists of members of the families $(x - c_1\tau = \text{const.})$ and $(x + c_1\tau = \text{const.})$. The diamond-shaped elements formed by this grid have diagonals measuring $2\Delta x$ and $2\Delta\tau$. The secondary set(s*) of grid lines consists of members of the families $x \pm c_2\tau = \text{const.}$

($x \pm c_3\tau$ = const.*). They are shown dotted in Fig. 9 and are used when analyzing an individual element.

To establish $\left\{ v_j\left(\frac{32\delta}{a}, \tau_m\right)\right\}$ we explore the nodal points along the characteristic lines $x - c_1\tau$ = const. in exactly the same manner as described for membrane theory. Only the technique for calculating (v_j) at the apex of a diamond-shaped element differs. For $m \leq 2$ the technique is identical to that used by McNiven and Mengi [1].

In explaining the general technique employed for $m > 2$ we refer to element M shown in Fig. 9 and to the enlargement. The vector (v_j) is known at points A_4 and A_5 located on the a^{th} characteristic; at points B_2, B_3, and B_4 on the b^{th} characteristic; and at points C_1 and C_2 on the c^{th} characteristic. We seek to establish (v_j) at the point C_3 situated on the c^{th} characteristic. As there are six (nine*) unknown components of the vector (v_j) we need six (nine*) equations.

Through the point C_3 we draw the characteristic lines C_3D_1 and C_3D_2 with slopes $\pm c_2$ (the characteristic lines C_3D_3 and C_3D_4 with slopes $\pm c_3$*). The values of (v_j) at D_1 (D_3*) are calculated by quadratic interpolation of the values at C_2, B_3, and A_4, and at D_2 (D_4*) by quadratic interpolation of the values at B_2, B_3, and B_4. Four (six*) of the six (nine*) equations come from using the four (six*) canonical equations, Eqs. (46) (Eqs. (50)*) along the four (six*) characteristic lines C_2C_3, B_4C_3, D_1C_3, and D_2C_3 (D_3C_3 and D_4C_3*). The two (three*) remaining equations are Eqs. (48) (Eqs. (51)*) which are employed along the diagonal B_3C_3 (x = const.). The six (nine*)

components of the vector (v_j) at C_3 are found by solving the six (nine*) equations by the method of finite differences.

For an element L adjacent to the line $x = 0$, the procedure must be modified in two ways. First, the value of the vector (v_j) at D_2 (D_4*) is calculated by quadratic interpolation of the values of (v_j) at B_1, B_2, and B_3. Secondly, the two (three*) canonical equations along the two (three*) characteristic lines $x - c_i\tau = \text{const.}$ $(i = 1,2 \ (3^*))$ are replaced by the boundary conditions at $x = 0$. From Eqs. (49) (Eqs. (54)*) these conditions are

$$\frac{\delta}{a} w_{,x}(C_1) = f_1(C_1)$$
$$u_{,x}(C_1) = 0 \quad . \tag{56}$$

V. COMPARISON OF PREDICTED AND EXPERIMENTAL RESPONSES

Experimental data was obtained from tests conducted by Kolsky and Heimann on cold drawn steel tubes. Identification of the mechanical properties of the steel was not contained within their paper, nor are the properties now known. As the theoretical solution is dependent on the mechanical properties of the specimen, it is necessary to ascertain these properties, specifically modulus of elasticity and Poisson's ratio, from the data that is available.

Steel tables provide upper and lower bounds for Poisson's ratio and modulus of elasticity for cold drawn steel. From these bounded sets, the values of 0.275 for Poisson's ratio and 28.2×10^3 ksi for modulus of elasticity are determined for the material by matching the peak of each of the theoretical strain responses (ε_{zz} and $\varepsilon_{\theta\theta}$) at station two, as calculated by membrane theory, to the corresponding peak of the experimental strain responses for $a^* = 1.03$. We assume that the same material properties apply to both specimens.

The decision to use only the experimental results of the thinner tube, $a^* = 1.03$, for the determination of the material properties is based on the amount of computer time required for a theoretical solution. Membrane theory requires significantly less time than either two-mode or three-mode theory. As membrane theory is restricted in use to thin shells, it is necessary to use a specimen that falls within the domain of applicability of this theory. The tube with $a^* = 1.03$, radius/thickness ratio of 32 is, therefore, chosen.

The longitudinal and hoop strain responses at station two for $a^* = 1.03$ as predicted by membrane theory are shown in Fig. 10 and Fig. 11 respectively. No attempt is made to obtain similar strain responses using two-mode and three-mode theories. The large value of b/h for this tube suggests that little improvement, if any, can be made over the membrane solution. Considering the complex nature of the experimental time dependencies at stations one and two and the significant differences in the two time dependencies, one is impressed by how well the theoretical predictions match the experimental responses at station two.

Figures 12 and 13 show the longitudinal and hoop strain responses at station two for $a^* = 1.15$, $b/h = 7.5$, as predicted by each of the three approximate theories. It can be seen from these figures that the three approximate solutions match the experimental results exceedingly well. The fact that not one of the approximate theories is noticeably better than another is not unexpected. First, an a^* of 1.15 is probably in the region between those values for which membrane theory is adequate and those values which require a more refined theory. Secondly, there is a trade-off of advantages when a higher order theory is used. The improvement introduced by a higher order theory in more closely reproducing exact behavior is somewhat offset by complications and sources of error that are introduced by the numerical procedure.

In contrast to membrane theory, two-mode and three-mode theories contain more than one wave front which necessitates the use of interpolations within the numerical procedure for calculation of

the vector (v_j) at the apex of each diamond-shaped element. As the responses at a considerable distance from the input are being sought, the effect of the interpolations and the accumulative errors generated by the interpolations is twofold. First, the amount of computer time required for a satisfactory solution is significantly increased. Smaller mesh sizes (in conjunction with a second order interpolation function, Section IV) are employed with the higher order theories in order to ensure the stability of the numerical procedure. Secondly, the rate at which the numerical solutions converge is reduced.

On the basis of the results shown here, we speculate that, as the value of a* increases, somewhat beyond 1.15, the two-mode theory would supply a predicted response much closer to the experimental behavior than that predicted by membrane theory. Also, it seems entirely likely that as a* is further increased, it will reach a value for which the three-mode theory would be an improvement over the two-mode theory.

Finally, one can conclude that the method of characteristics is valuable in calculating responses to a transient input on the end of a hollow rod at least when the response is no farther from the disturbance than that considered here.

REFERENCES

1. Y. Mengi and H. D. McNiven, "Analysis of the Transient Excitation of an Elastic Rod by the Method of Characteristics," International Journal of Solids and Structures, Vol. 6, 1970, pp. 871 - 892.

2. Sing - Chih Tang, "A Solution of the Partial Differential Equations Governing Vibration of a Rod," American Institute of Aeronautics and Astronautics Journal, Vol. 3, 1965, pp. 1174 - 1175.

3. J. H. Heimann and H. Kolsky, "The Propagation of Elastic Waves in Thin Cylindrical Shells," Journal of Mechanics and Physics of Solids, Vol. 14, 1966, pp. 121 - 130.

4. J. H. Heimann, "An Investigation of Wave Propagation in Hollow Tubes," Brown University Report, Division of Appl. Math., ARPA/AM - 10, 1964.

5. H. D. McNiven, A. H. Shah, and J. L. Sackman, "Axially Symmetric Waves in Hollow, Elastic Rods: Part I," Journal of Acoustical Society of America, Vol. 40, 1966, pp. 784 - 792.

6. R. D. Mindlin and G. Herrmann, "A One-Dimensional Theory of Compressional Waves in an Elastic Rod," Proceedings of the First U. S. National Congress of Applied Mechanics, June, 1951 (American Society of Mechanical Engineers, New York, 1952), pp. 187 - 191.

7. R. D. Mindlin and H. D. McNiven, "Axially Symmetric Waves in Elastic Rods," Journal of Applied Mechanics, Vol. 82, 1960, pp. 145 - 151.

8. R. Courant and D. Hilbert, "Method of Mathematical Physics, Vol. II," Interchange Publishers, 1966.

9. Y. Mengi and H. D. McNiven, "Dispersion of Cylindrical Waves in a Viscoelastic Body," to be published in the International Journal of Solids and Structures.

CAPTIONS FOR FIGURES

Fig. 1 Comparison between the exact and membrane frequency spectra for $a^* = 1.03$.

Fig. 2 Comparison between the exact and membrane frequency spectra for $a^* = 1.15$.

Fig. 3 Comparison between the exact and two-mode frequency spectra for $a^* = 1.03$.

Fig. 4 Comparison between the exact and two-mode frequency spectra for $a^* = 1.15$.

Fig. 5 Comparison between the exact and three-mode frequency spectra for $a^* = 1.03$.

Fig. 6 Comparison between the exact and three-mode frequency spectra for $a^* = 1.15$.

Fig. 7 Experimental longitudinal strain responses at station one.

Fig. 8 Characteristic lines and wave front on the $(x - \tau)$ plane for membrane theory.

Fig. 9 Characteristic lines and wave fronts on the $(x - \tau)$ plane for two-mode and three-mode theories.

Fig. 10 Comparison between the experimental longitudinal strain responses at station two for $a^* = 1.03$ and the response predicted by membrane theory.

Fig. 11 Comparison between the experimental hoop strain response at station two for $a^* = 1.03$ and the response predicted by membrane theory.

Fig. 12 Comparison between the experimental longitudinal strain response at station two for $a^* = 1.15$ and the responses predicted by the three approximate theories.

Fig. 13 Comparison between the experimental hoop strain response at station two for $a^* = 1.15$ and the responses predicted by the three approximate theories.

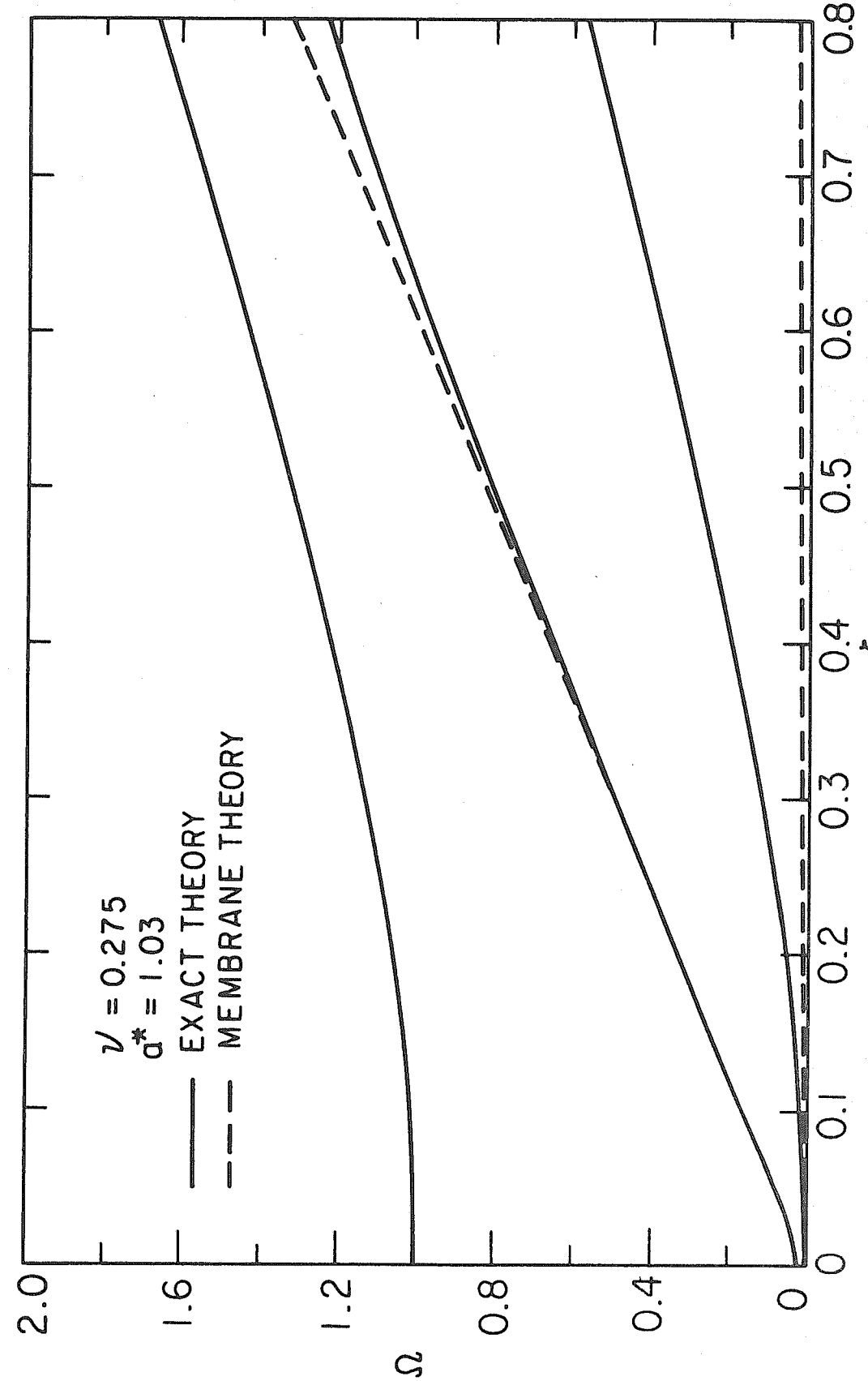
ν = 0.275
a* = 1.03
EXACT THEORY
MEMBRANE THEORY
Ω
ζ
0
0.4
0.8
1.2
1.6
2.0
0.1
0.2
0.3
0.4
0.5
0.6
0.7
0.8

FIG. 1

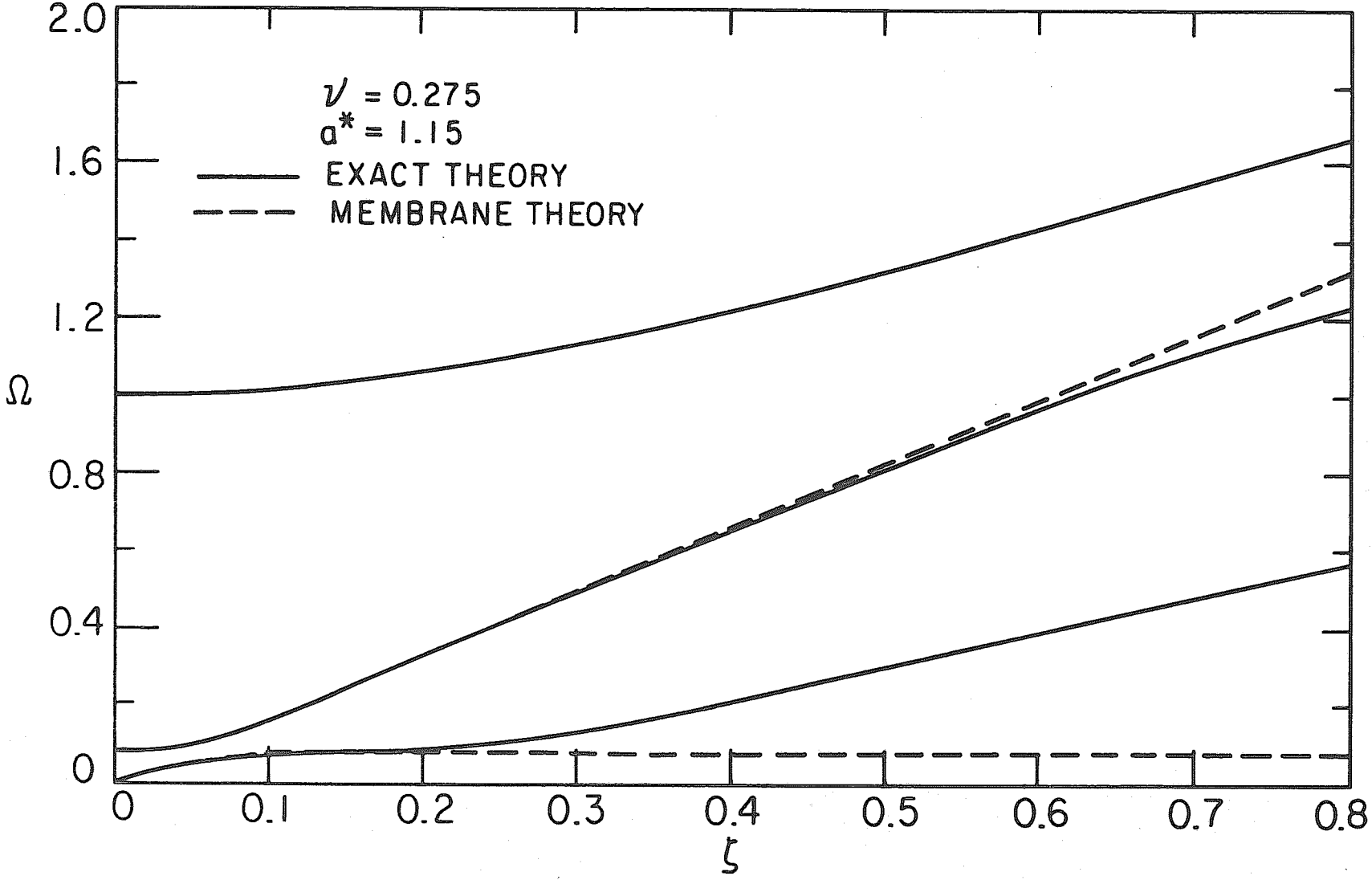
2.0
1.6
1.2
0.8
0.4
0
Ω
ν = 0.275
a* = 1.15
EXACT THEORY
MEMBRANE THEORY
0
0.1
0.2
0.3
0.4
0.5
0.6
0.7
0.8
ζ

FIG. 2

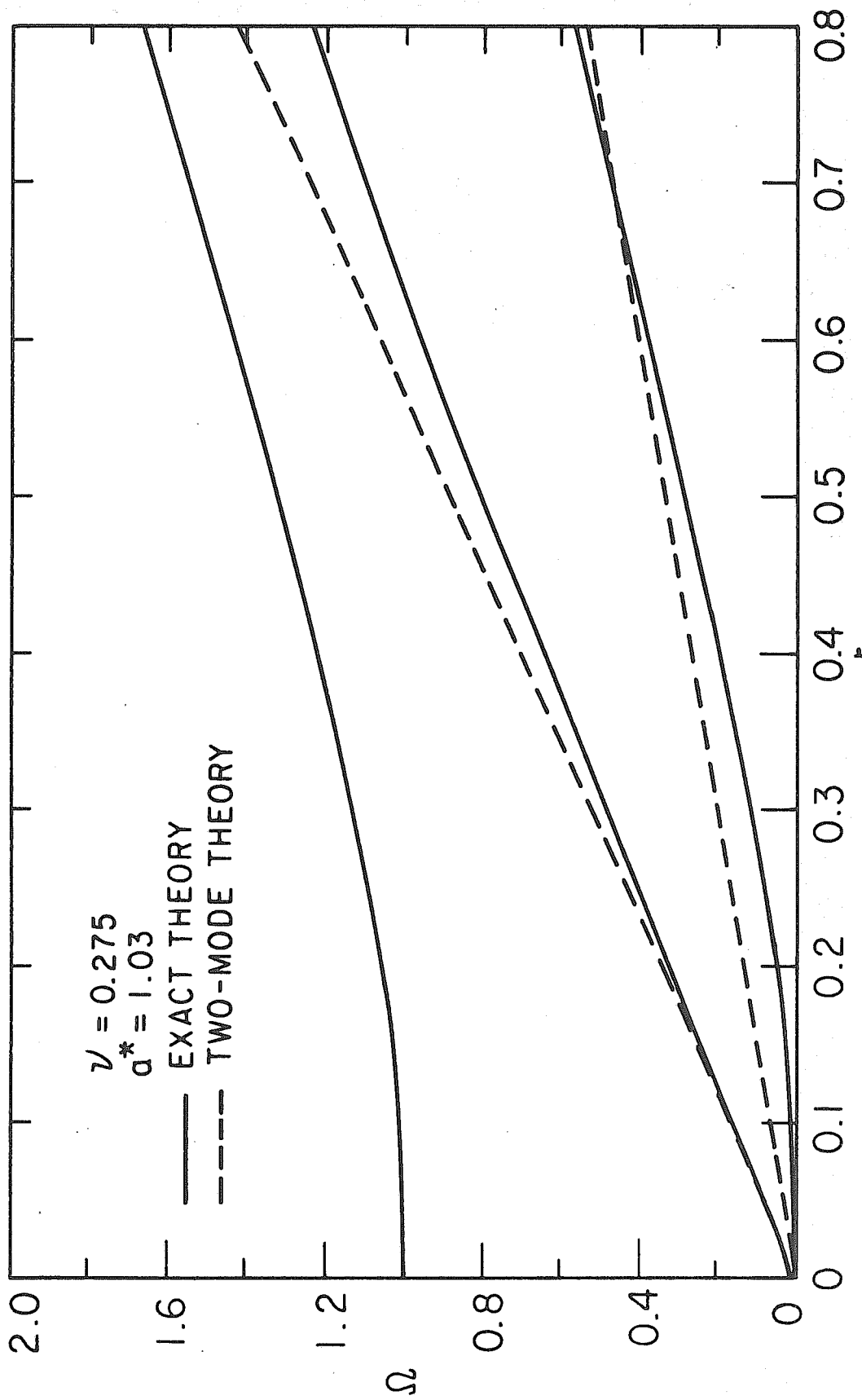
ν = 0.275
a* = 1.03
EXACT THEORY
TWO-MODE THEORY
Ω
ζ
2.0
1.6
1.2
0.8
0.4
0
0.1
0.2
0.3
0.4
0.5
0.6
0.7
0.8

FIG. 3

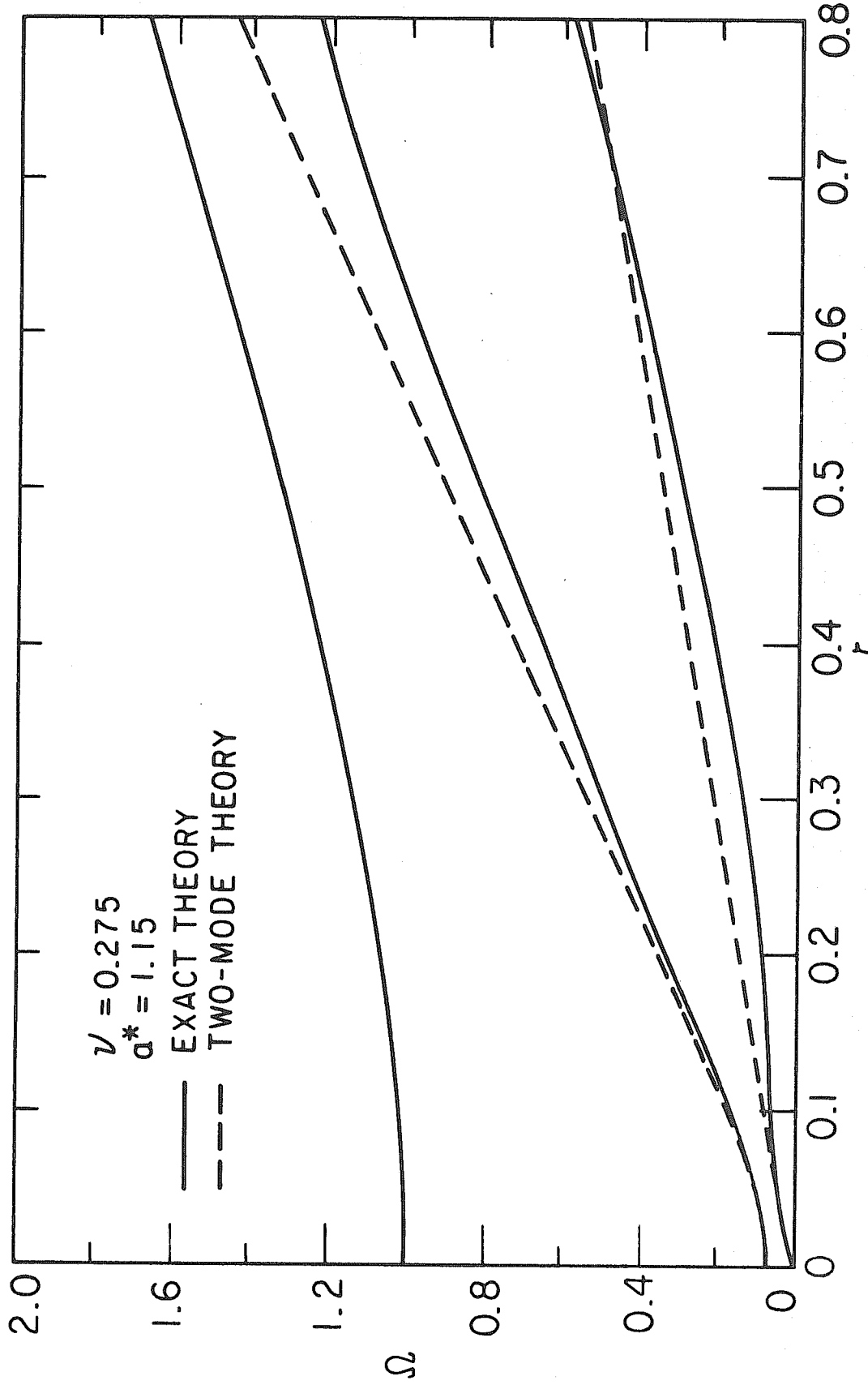
ν = 0.275
a* = 1.15
EXACT THEORY
TWO-MODE THEORY
Ω
ζ
0
0.4
0.8
1.2
1.6
2.0
0.1
0.2
0.3
0.4
0.5
0.6
0.7
0.8

FIG. 4

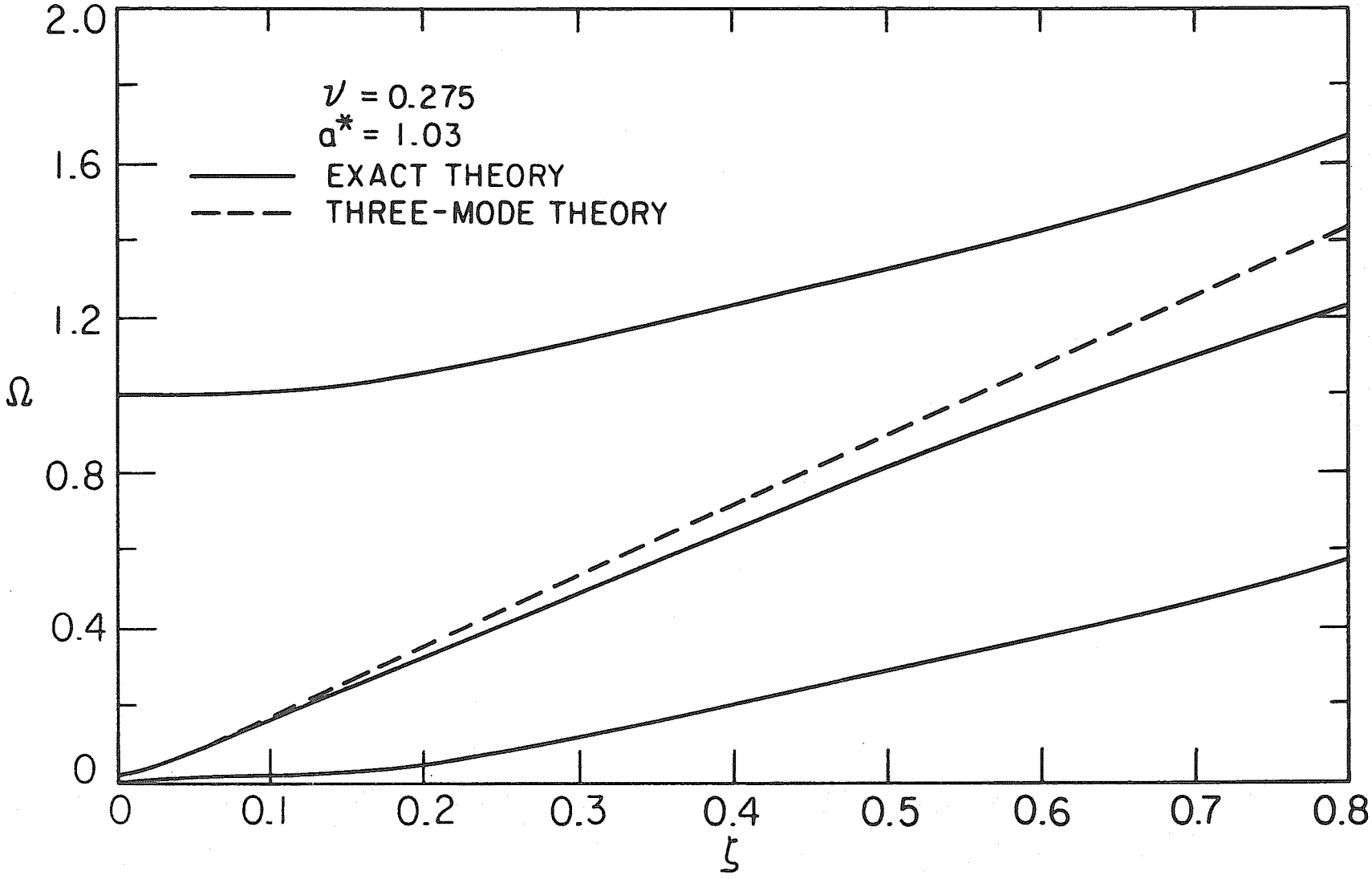
2.0
1.6
1.2
0.8
0.4
0
Ω
ν = 0.275
a* = 1.03
EXACT THEORY
THREE-MODE THEORY
0
0.1
0.2
0.3
0.4
0.5
0.6
0.7
0.8
ζ

FIG. 5

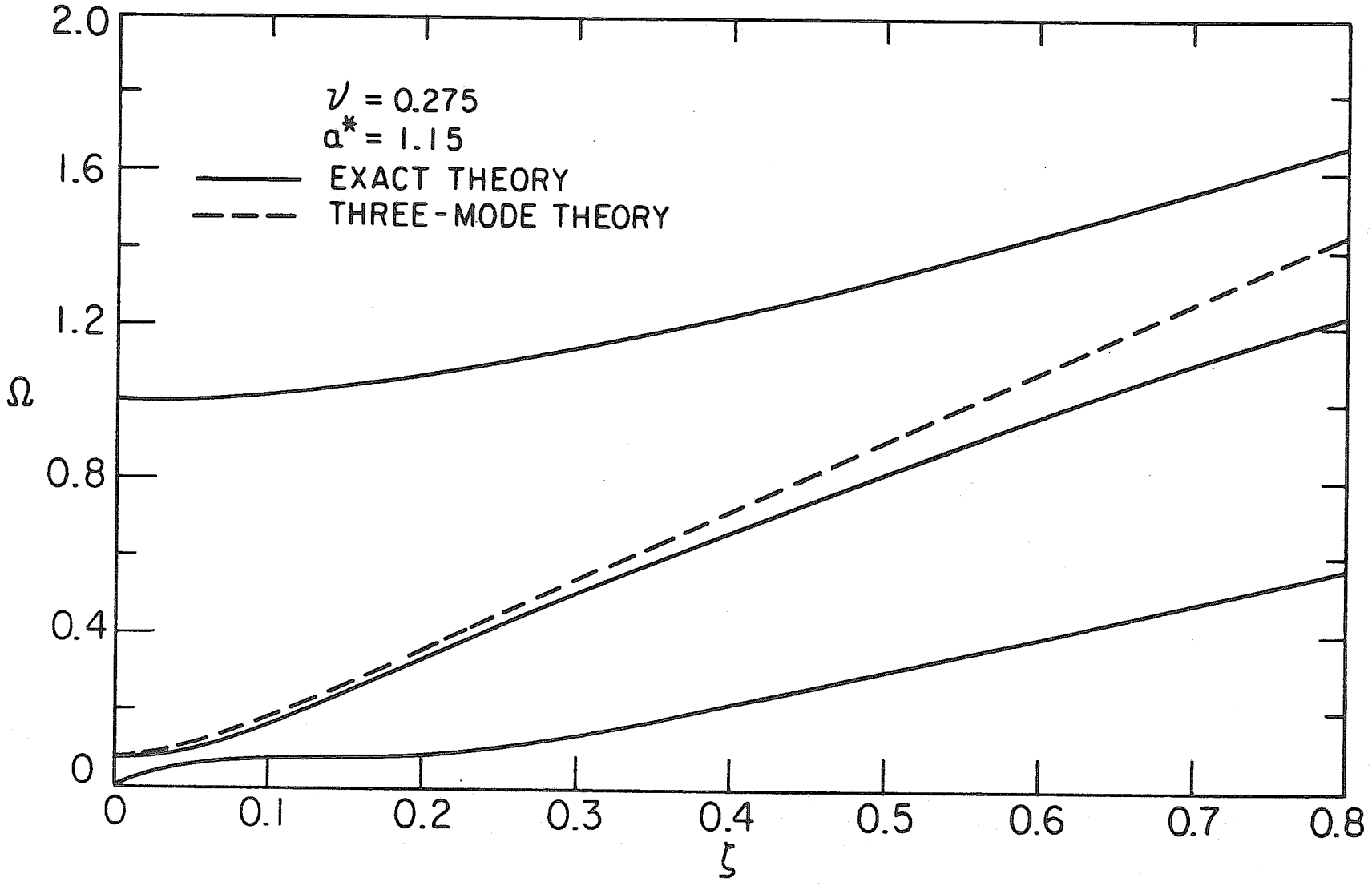
2.0
1.6
1.2
0.8
0.4
0
Ω
ν = 0.275
a* = 1.15
EXACT THEORY
THREE-MODE THEORY
0
0.1
0.2
0.3
0.4
0.5
0.6
0.7
0.8
ζ

FIG. 6

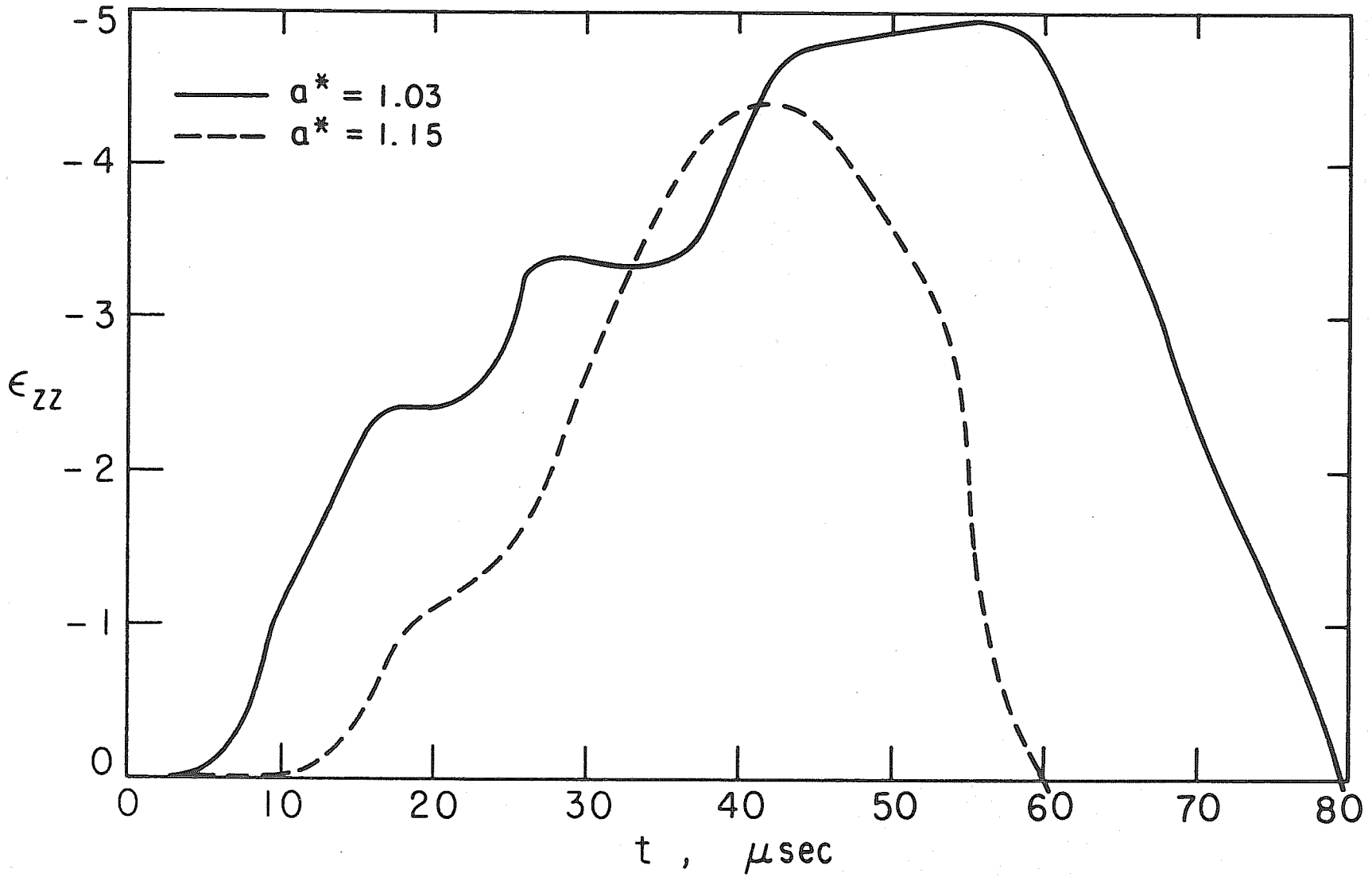

FIG. 7

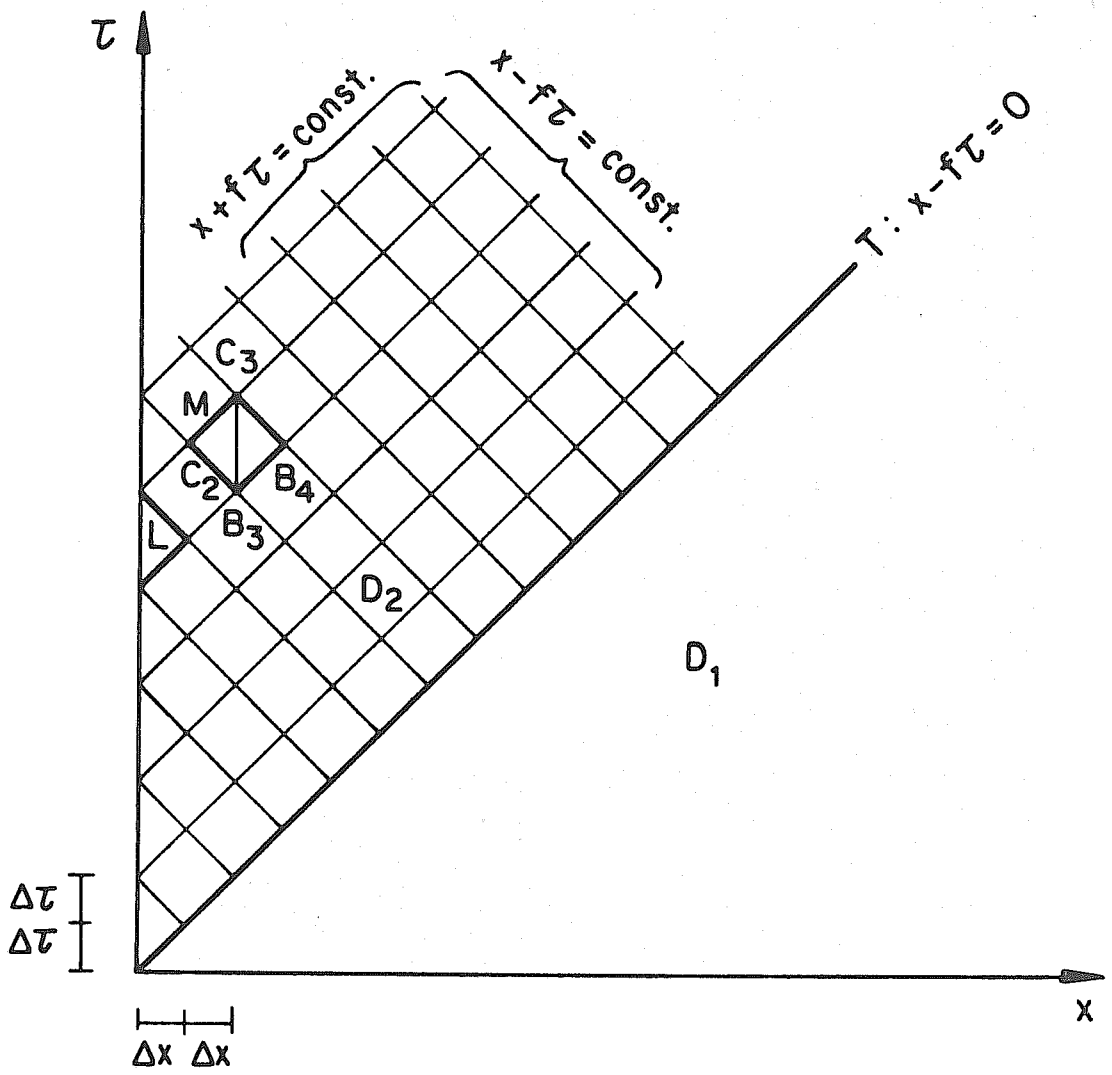

FIG. 8

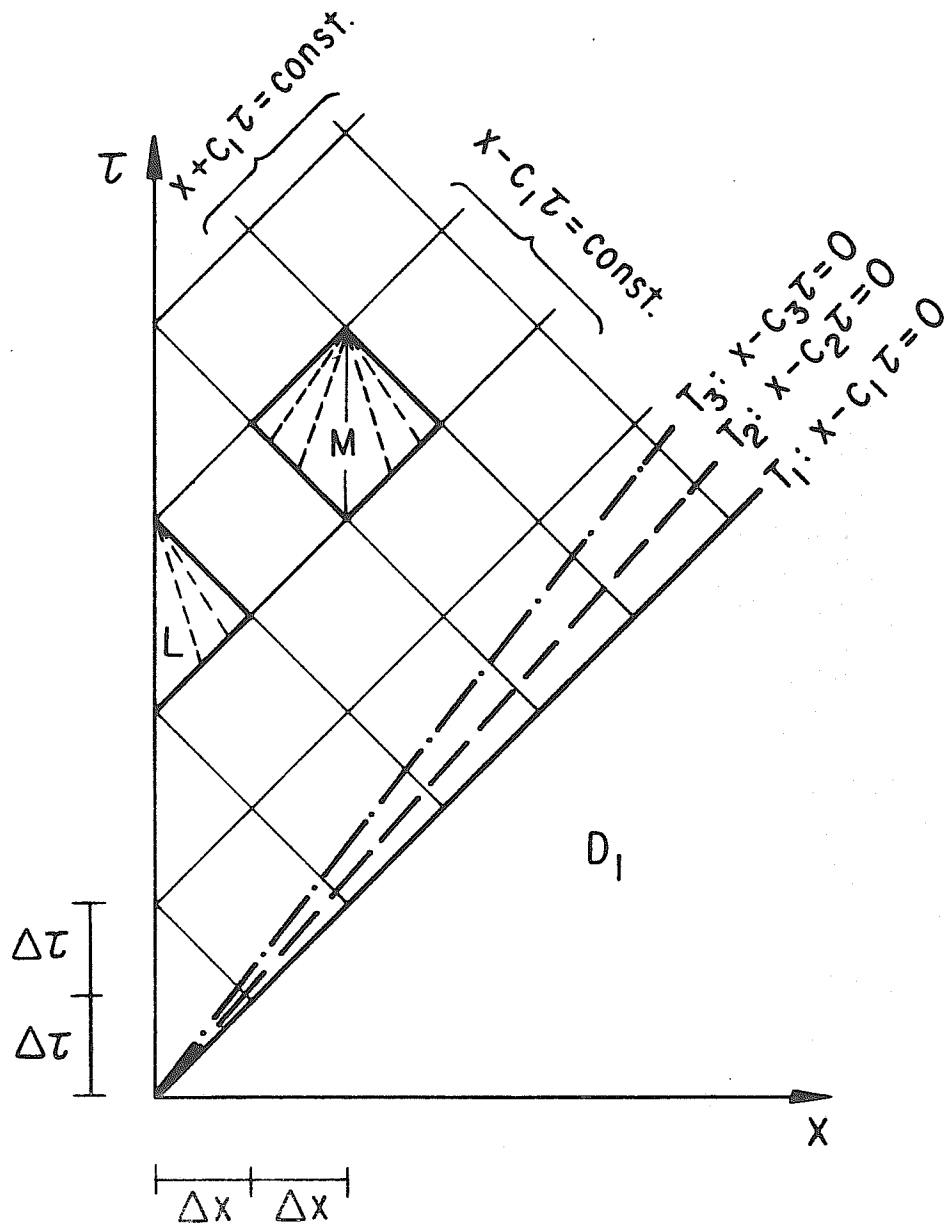

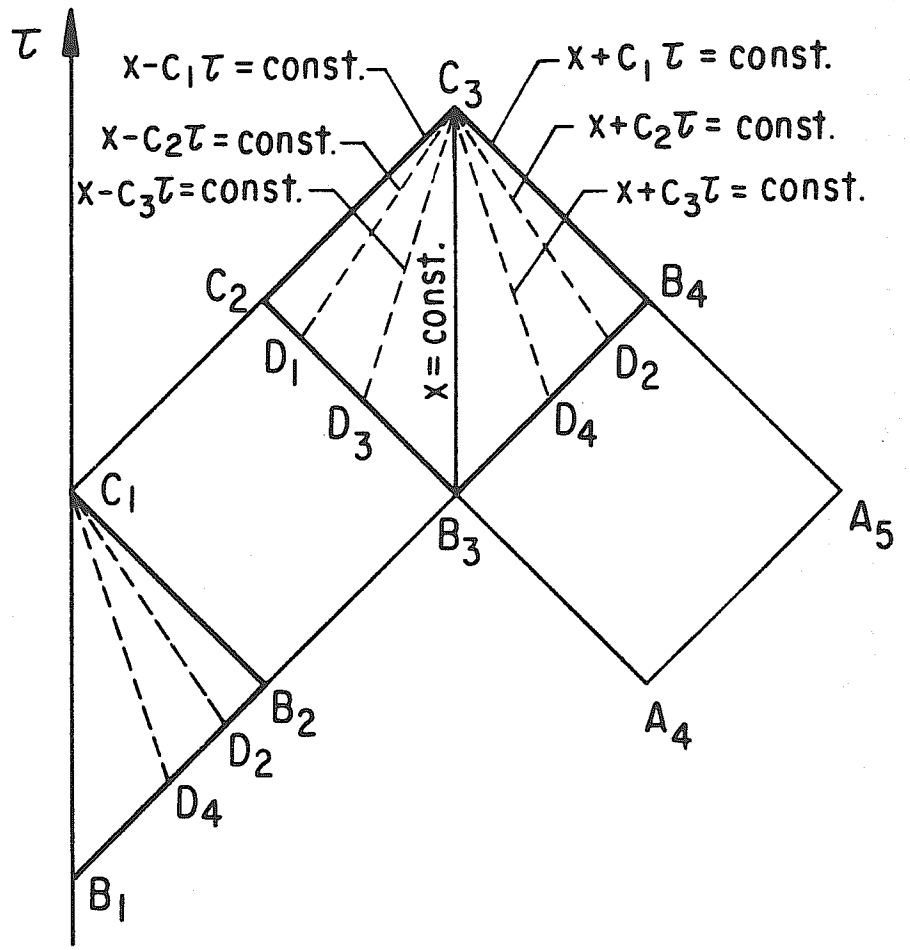

DETAIL OF ELEMENTS M AND L

FIG. 9

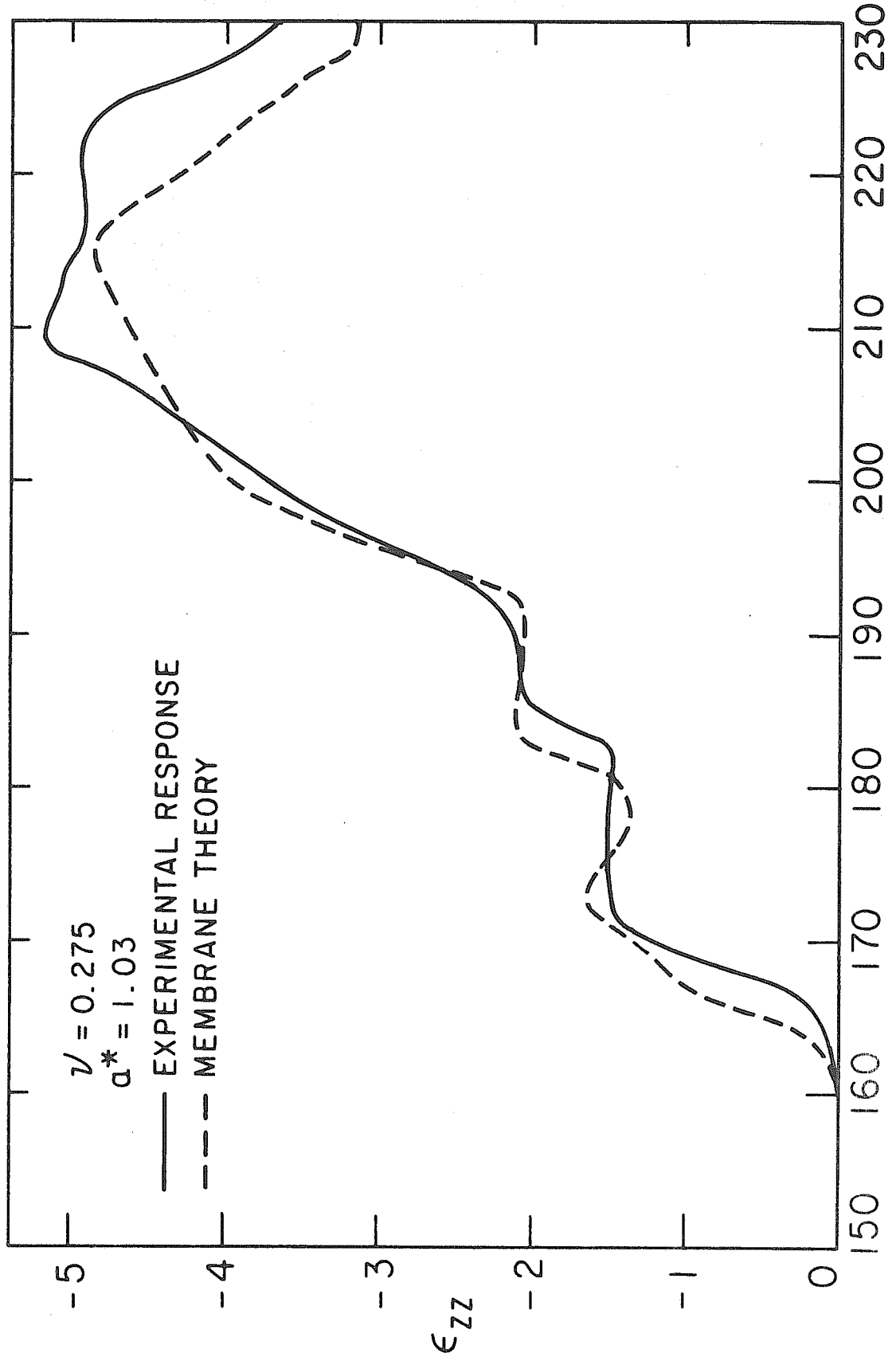
$\nu = 0.275$
$a^* = 1.03$
EXPERIMENTAL RESPONSE
MEMBRANE THEORY
ϵ_{zz}
-5
-4
-3
-2
-1
0
150
160
170
180
190
200
210
220
230
t , μsec

FIG. 10

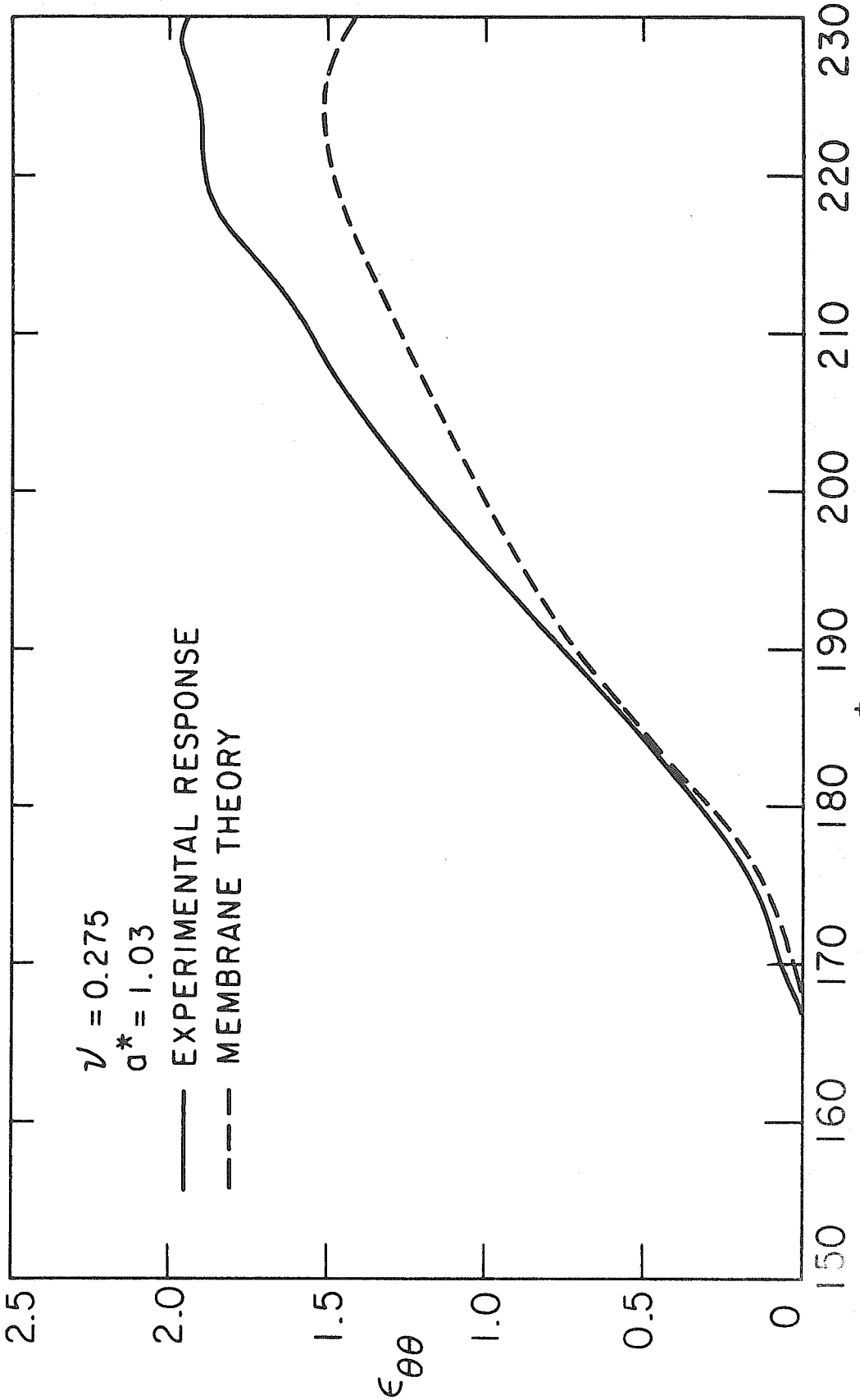
2.5
2.0
1.5
1.0
0.5
0
$\epsilon_{\theta\theta}$
150
160
170
180
190
200
210
220
230
t , μsec
ν = 0.275
a* = 1.03
EXPERIMENTAL RESPONSE
MEMBRANE THEORY

FIG. 11

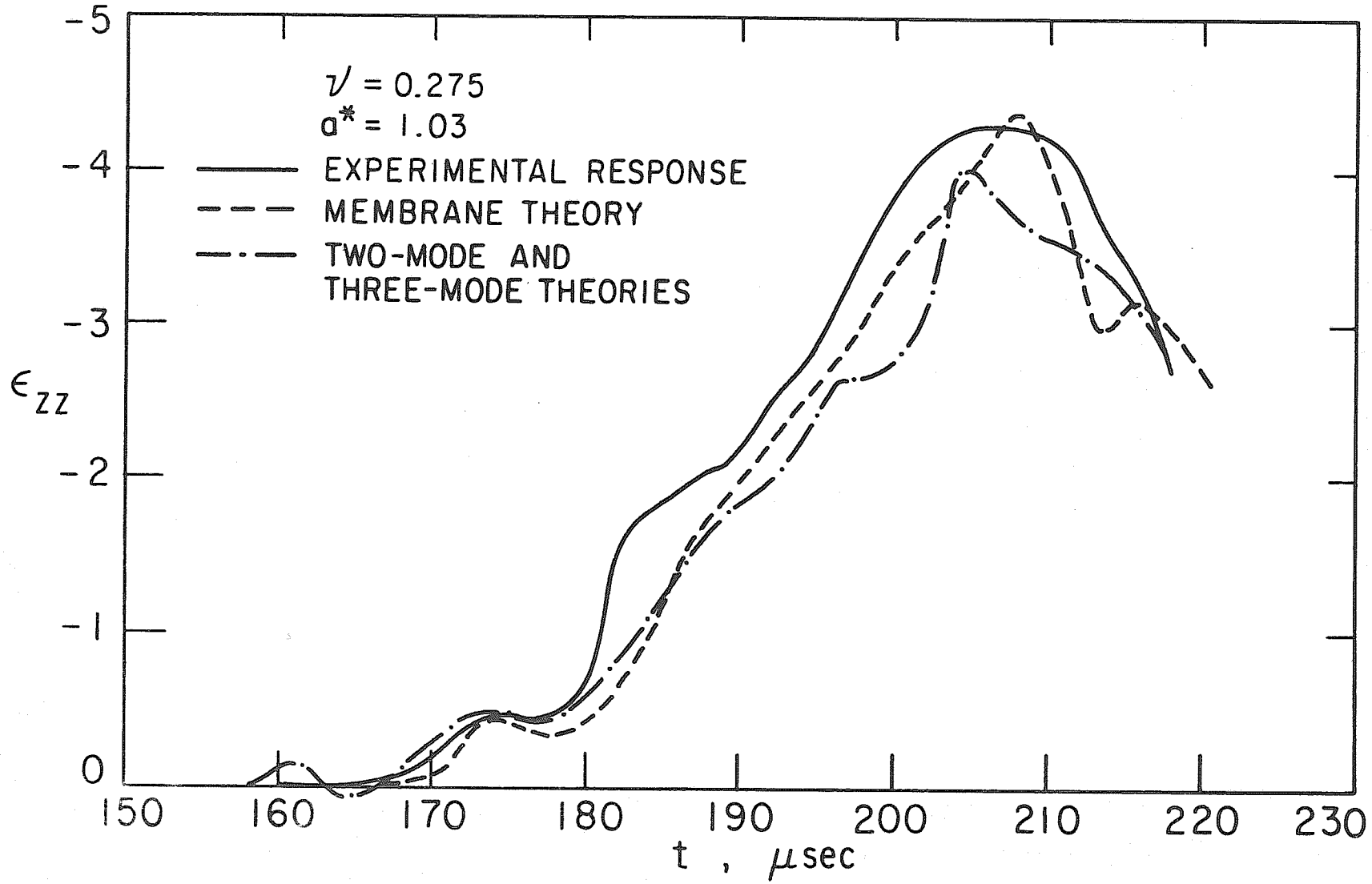
-5
-4
-3
-2
-1
0
ϵ_{zz}
$\nu = 0.275$
$a^* = 1.03$
EXPERIMENTAL RESPONSE
MEMBRANE THEORY
TWO-MODE AND
THREE-MODE THEORIES
150
160
170
180
190
200
210
220
230
t , μsec

FIG. 12

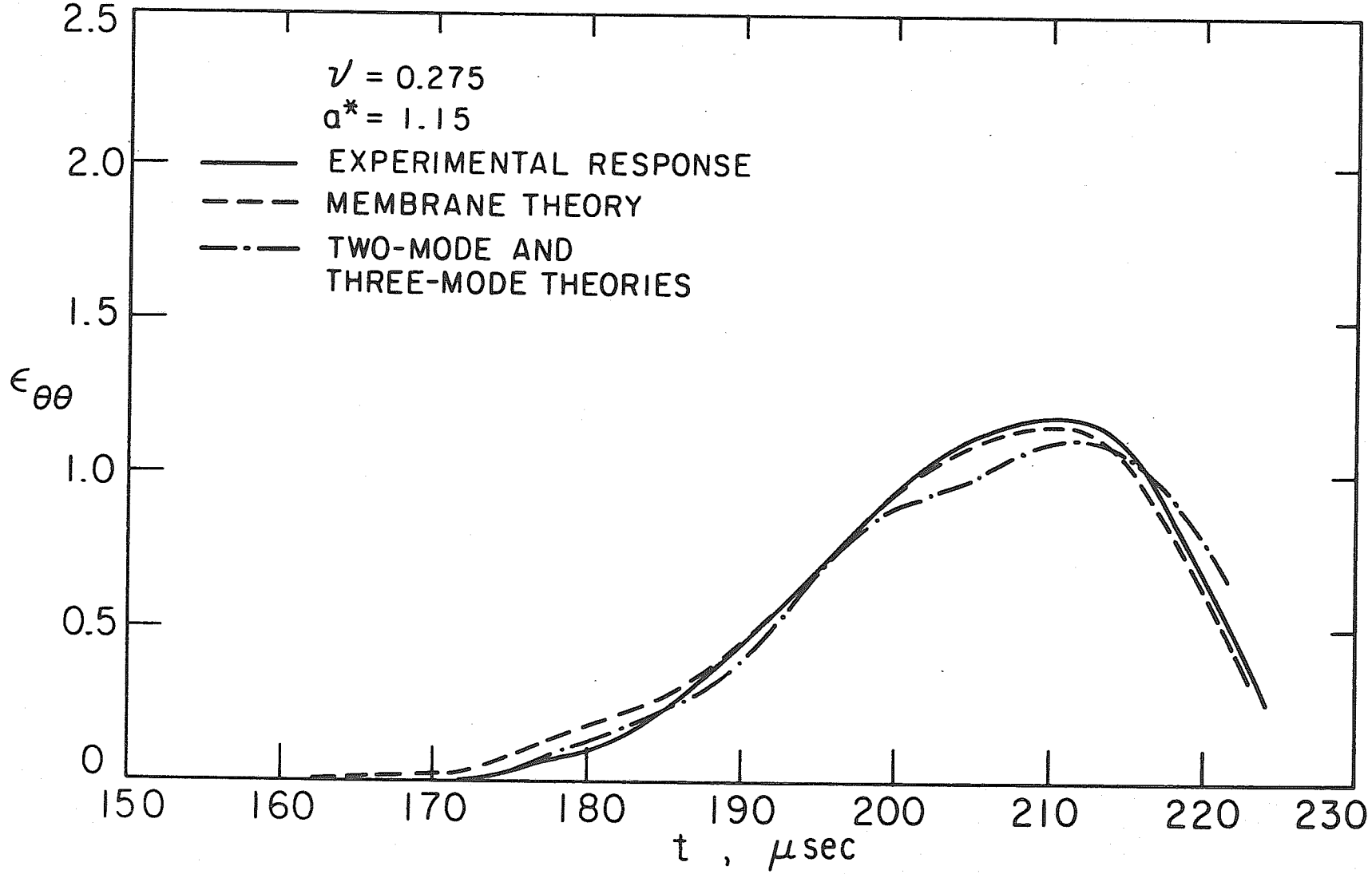
2.5
2.0
1.5
1.0
0.5
0
$\epsilon_{\theta\theta}$
ν = 0.275
a^* = 1.15
EXPERIMENTAL RESPONSE
MEMBRANE THEORY
TWO-MODE AND
THREE-MODE THEORIES
150
160
170
180
190
200
210
220
230
t , μsec

FIG. 13